Transition from the adiabatic to the sudden limit in core-electron photoemission

Lars Hedin and John Michiels
MPI-FKF, Heisenbergstrasse 1, D-70569 Stuttgart, Germany

John Inglesfield
University of Wales, Cardiff, P.O. Box 913, Cardiff CF2 3YB, United Kingdom
(Received 17 July 1998; revised manuscript received 3 September 1998)

Experimental results for core-electron photoemission $J_{\mathbf{k}}(\omega)$ are often compared with the one-electron spectral function $A_c(\epsilon_k-\omega)$, where ω is the photon energy, ϵ_k is the photoelectron energy, and the optical transition matrix elements are taken as constant. Since $J_{\mathbf{k}}(\omega)$ is nonzero only for $\epsilon_k>0$, we must actually compare it with $A_c(\epsilon_k-\omega)\theta(\epsilon_k)$. For metals $A_c(\omega)$ is known to have a quasiparticle (QP) peak with an asymmetric power-law [theories of Mahan, Nozières, de Dominicis, Langreth, and others (MND)] singularity due to low-energy particle-hole excitations. The QP peak starts at the core-electron energy ϵ_c, and is followed by an extended satellite (shakeup) structure at smaller ω. For photon energies ω just above threshold, $\omega_{th}=-\epsilon_c$, $A_c(\epsilon_k-\omega)\theta(\epsilon_k)$ as a function of ϵ_k (ω constant) is cut just behind the quasiparticle peak, and neither the tail of the MND line nor the plasmon satellites are present. The sudden (high-energy) limit is given by a convolution of $A_c(\omega)$ and a loss function, i.e., by the Berglund-Spicer two-step expression. Thus $A_c(\omega)$ alone does not give the correct photoelectron spectrum, neither at low nor at high energies. We present an extension of the quantum-mechanical (QM) models developed earlier by Inglesfield, and by Bardyszewski and Hedin to calculate $J_{\mathbf{k}}(\omega)$. It includes recoil and damping, as well as shakeup effects and extrinsic losses, is exact in the high-energy limit, and allows calculations of $J_{\mathbf{k}}(\omega)$ including the MND line and multiple plasmon losses. The model, which involves electrons coupled to quasibosons, is motivated by detailed arguments. As an illustration we have made quantitative calculations for a semi-infinite jellium with the density of aluminum metal and an embedded atom. The coupling functions (fluctuation potentials) between the electron and the quasibosons are related to the random-phase-approximation dielectric function, and different levels of approximations are evaluated numerically. The differences in the predictions for the photoemission spectra are found small. We confirm the finding by Langreth that the BS limit is reached only in the keV range. At no photon energy are the plasmon satellites close to being either purely intrinsic or extrinsic. For photoelectron energies larger than a few times the plasmon energy, a semiclassical approximation gives results very close to our QM model. At lower energies the QM model gives a large peak in the ratio between the total intensity in the first plasmon satellite and the main peak, which is not reproduced by the SC expression. This maximum has a simple physical explanation in terms of different dampings of the electrons in the QP peak and in the satellite. For the MND peak $J_{\mathbf{k}}(\omega)$ and $A_c(\epsilon_k-\omega)$ agree well for a range of a few eV, and experimental data can thus be used to extract the MND singularity index. For an embedded atom at a small distance from the surface there are, however, substantial deviations from the large-distance limit. Our model is simple enough to perform quantitative calculations allowing for band-structure and surface details. [S0163-1829(98)03847-8]

I. INTRODUCTION

Photoemission spectroscopy (PES) has become an important tool for studying properties of matter. Most measurements have aimed at obtaining electron band structures, i.e., electron quasiparticle energies. The experimental results are generally in good agreement with theory for large classes of systems. The interpretation of experiment is mostly based on the *sudden approximation*, expressing PES in terms of the one-electron spectral function $A(\omega)$. There is, however, never a true correspondence between PES and $A(\omega)$, not even at high energies. The reason is that $A(\omega)$ only describes the primary excitation of the photoelectron, but does not take account of the losses the photoelectron can have before it leaves the solid. This has been recognized from the start of the field, and the earliest attempts to account for this discrepancy was the use of the Berglund-Spicer (BS) three-step model.[1] Apart from the surface losses, the BS model simply means a convolution of the spectral function $A(\omega)$ with a loss function. Such a convolution does not change the *position* of a sharp quasiparticle peak. Quasiparticle peaks, however, have a lifetime width, and the experimental width is thus not the same as the width of the peak in $A(\omega)$. They also have an asymmetry, which has to be known to allow a precise assignment of a peak position.

Besides the quasiparticle peak, $A(\omega)$ has an incoherent satellite structure. In sp solids the satellite structure is mainly due to shakeup of surface and bulk plasmons. In high-T_c materials the incoherent background can be associated with, e.g., spin excitations, and gives important information regarding the nature of the electronic correlation. The spectral function is also influenced by thermal motion, i.e., it gives information on phonon properties. With synchrotron radiation sources the resolution in PES has been vastly improved, and the data now show a richness in detail besides peak positions, which demands a comprehensive theoretical interpretation.

The satellite structures in PES originate both from $A(\omega)$ and from the losses the photo-electron can have before it leaves the solid. We talk about *intrinsic* [coming from $A(\omega)$] and *extrinsic* losses. Between these two types of losses there is quantum-mechanical interference. This interference results in a strong suppression of the satellite structures as compared to the BS predictions, up to photoelectron energies in the keV region. When the interferences are gone, and the BS model applies, we may say that we are in the *sudden limit*, since we only have to convolute $A(\omega)$ with a loss function to get the PES spectrum. At threshold, when we may say that we are in the *adiabatic limit*, the satellites are absent due to energy conservation. Qualitatively we can consider the adiabatic limit in time development and use a semiclassical picture. The combined effect of the potential from the hole left by the photoelectron and the slowly moving photoelectron gives a slowly varying potential to which the solid adjusts adiabatically. This picture is, however, not possible to quantify, and at low energies the semiclassical approximation is quantitatively poor, as we will discuss later in this paper.

Since the mean free path is typically 5–20 Å it is clear that the surface plays an essential role for PES. This makes any theory beyond the BS model complicated. This paper has a twofold purpose, namely, to quantitatively describe the transition from the adiabatic to the sudden limit in core-electron PES in a simple model situation, and to develop a method that allows quantitative calculations of more realistic systems.

A general approach to PES was developed by Caroli *et al.*[2] and Chang and Langreth[3] based on Keldysh diagrams, which has been further expanded by, among others, Bose, Longe, and collaborators,[4] and Almbladh.[5] Here we will use a different, and more elementary approach than by use of Keldysh diagrams.[6,7] We use an electron-boson Hamiltonian, where both the photoelectron and the core electron are coupled to bosonic-type excitations in the solid via fluctuation potentials. We then make a straightforward perturbation expansion in terms of the fluctuation potentials $V^{\mathbf{q}}(\mathbf{r})$ (cf. Sec. III), rather than in a dynamically screened Coulomb potential $W(\mathbf{r},\mathbf{r}';\omega)$. Note that the $V^{\mathbf{q}}(\mathbf{r})$ are functions only of $\mathbf{r}$ and not of $\mathbf{r}$ and $\mathbf{r}'$, and do not depend on ω. We study only core-electron PES, which is considerably simpler than valence electron PES. Our approach is fully quantum mechanical (QM), and, e.g., the recoil of the photoelectron and its damping are considered.

The fluctuation potentials can be obtained from the dielectric function. Our lowest-order approximation for the photocurrent is quadratic in the fluctuation potentials, and can be expressed in terms of the dielectric function.

A central issue is a good treatment of the fluctuation potentials corresponding to the random-phase-approximation (RPA) dielectric function. This function was discussed in detail by Newns[8] for a semi-infinite jellium. The RPA function is, however, quite complicated, and a simpler version, corresponding to an infinite barrier and specular reflection of the electrons, is often used. In this approximation, which neglects interference between incoming and reflected electrons, only the jellium *bulk* dielectric function is involved. The screened interaction corresponding to this approximation has been written in analytical form by Bechstedt, Enderlein, and Reichardt,[9] and we have further obtained the corresponding fluctuation potentials. Inglesfield[6,10] has used further simplified fluctuation potentials, which turn out to give results closely similar to those of Bechstedt. Other estimates of electron-solid coupling functions were discussed by, e.g., Feibelman, Duke, and Bagchi,[11] and by Eguiluz.[12] An important issue in our paper is that we are not restricted to plasmon-pole-type approaches, but have obtained results also with the RPA dielectric function including electron-hole excitations.

An even simpler approach is the semiclassical (SC) one, where the photoelectron is put on a trajectory and not allowed to recoil. This approach is old and it is hard to trace its origin. It was used early in the classic paper by Lindhard,[13] and it has been used by Ferrell[14] to discuss plasmon satellites in x-ray emission. A detailed discussion, directly relevant for this paper, was given by Lucas, Kartheuser, and Badro[15] for electron-phonon scattering, and accounted very successfully for experimental data.

An approach related to the SC one is due to Simonsen, Yubero, and Tougaard.[16] Here the dielectric response of the system is found from a theory by Garcia-Moliner and Rubio (see, e.g., Ref. 17) involving pseudosurface charges.

The main results in this paper are the following. We derive the high-energy limit of PES, and find arguments as to why the photoelectron-solid coupling should be given by a fluctuation potential. We find a relation between the fluctuation potentials and the imaginary part of the RPA expression for the dynamically screened potential, and check that our model electron-boson Hamiltonian reproduces the GW approximation[18] for the electron self-energy. We follow in detail, both analytically and numerically, how the transition from QM to SC and to BS takes place. Using the formal similarity between the QM, SC, and BS results, we generalize the results in Ref. 7 to a closed expression containing plasmon losses to all orders as well as the particle-hole losses. We find explicit analytic results for the fluctuation potentials in the case of a dielectric function of a semi-infinite jellium with an infinite potential barrier and specular reflection of the electrons at the surface. These analytic results are compared with those from a full RPA calculation.

Core electron PES is an old problem. The asymmetric quasiparticle line due to particle-hole and phonon shakeup has been treated extensively, and the results by Mahan, Nozieres, de Dominicis, Langreth, and others are discussed in textbooks (MND theory).[19] With our approach we find a power-law behavior set by intrinsic losses only, out to several eV from the edge. We further find that the MND x-ray edge singularity index is enhanced when the emitting electron is close to the surface, but quickly approaches its bulk value (within, say, approximately 5 a.u.). Our approach also reproduces multiple plasmon losses and the smooth background from electron-hole excitations.

The outline of this paper is as follows. First we discuss basic theory and derive the sudden approximation in Sec. II A. In Sec. II B a discussion follows on photoemission in the electron-boson model. We obtain general results to arbitrary order in the electron-boson coupling functions, the fluctuation potentials. The background for the electron-boson model is discussed in Appendix A, and the properties of the fluctuation potentials are derived in Appendix B. In Sec.

II C 1 detailed results for one-boson satellites are derived, and as an example, explicit results with the Inglesfield bulk plasmon potential are given in Sec. II C 2, as well as the high-energy and large-z_c limit in Sec. II C 3 (z_c is the distance of the core electron from the surface). In Sec. II D we generalize the one-boson loss results to an exponential form, which includes multiboson losses. The BS expression is written in a compact form in Sec. II E. The exact solution for the SC case, derived in Appendix C, is discussed in Sec. II F, and compared with the QM results. Finally in Sec. II we compare the SC approach with that of Tougaard (Sec. II G). Section III is devoted to the central quantities in our theory, the fluctuation potentials. First the general relation to the dynamically screened Coulomb potential, derived in Appendix B, is discussed in Sec. III A, and then the Inglesfield and the Bechstedt approximations are discussed in Secs. III B and III C. Finally in Sec. III, the RPA potential is considered (Sec. III D). In Sec. IV we present our results, and in Sec. V we give concluding remarks.

II. PHOTOEMISSION THEORY

A general expression for the photoelectron current can be obtained from scattering theory[20] (we use atomic units, $e=\hbar=m=1$, and thus, e.g., energies are in Hartrees, 27.2 eV),

$$J_{\mathbf{k}}(\omega)=\sum_s |\langle\Psi_{\mathbf{k},\mathbf{s}}|\Delta|\Psi_i\rangle|^2\delta(\omega-\varepsilon_{\mathbf{k}}+\varepsilon_s). \tag{1}$$

This is the standard golden rule expression with final states having the proper boundary conditions for scattering states. All states are correlated. Further, $\varepsilon_{\mathbf{k}}$ is the energy of the photo-electron, $\mathbf{k}^2/2$, ε_s gives the energy of the final state of the solid as $\varepsilon_s=E(N,0)-E(N-1,s)$, ω is the photon energy, and Δ is the optical transition operator, $\Delta=\Sigma_{ij}\langle i|Ap+pA|j\rangle c_i^\dagger c_j$. $|\Psi_i\rangle$ is the initial state, and $|\Psi_{\mathbf{k},\mathbf{s}}\rangle$ the final state, which can be written

$$|\Psi_{\mathbf{k},\mathbf{s}}\rangle=\left[1+\frac{1}{E-H-i\eta}(H-E)\right]c_{\mathbf{k}}^\dagger|N-1,s\rangle, \tag{2}$$

where H is the fully interacting Hamiltonian including target electrons and photoelectron, and $E=\omega+E(N,0)=\varepsilon_{\mathbf{k}}+E(N-1,s)$. $|N-1,s\rangle$ is the target state after the photoelectron has left, and $c_{\mathbf{k}}^\dagger$ creates the photoelectron. The states corresponding to $c_{\mathbf{k}}^\dagger$ are so far undefined, except that they are time-inverted LEED states with asymptotically a plane-wave part $\exp(i\mathbf{k}\cdot\mathbf{r})$. We will suppress spin variables.

A. Sudden approximation

In the sudden approximation the final state is approximated as $|\Psi_{\mathbf{k},\mathbf{s}}\rangle=c_{\mathbf{k}}^\dagger|N-1,s\rangle$. This means that all extrinsic interactions between the photoelectron and the target system are neglected. At high energies this is a good approximation for finite systems such as atoms and molecules, atoms on surfaces, etc. (with a proper choice of photoelectron states $\mathbf{k}$, see Appendix A), because the electron scattering rates go to zero with increasing energy. The sudden approximation is, however, never good for solids, and always has to be corrected for extrinsic losses. This is so because with increasing electron energy, the mean free path increases, and the electrons come from increasingly larger distances from the surface. Thus even though the scattering rate goes down, the total scattering tends to a constant, as shown in Sec. II E, Eq. (44).

From Eq. (1) it immediately follows that

$$J_{\mathbf{k}}(\omega)=\sum_s \left|\left\langle N-1,s\left|c_{\mathbf{k}}\sum_{ij}\Delta_{ij}c_i^\dagger c_j\Psi_i\right\rangle\right|^2\delta(\omega-\varepsilon_{\mathbf{k}}+\varepsilon_s).$$

If the photoelectron $\mathbf{k}$ is fast enough, there are no virtual states in $|\Psi_i\rangle$ to annihilate, and then $c_{\mathbf{k}}$ must match $c_i^\dagger$. This gives the well-known sudden approximation[21]

$$J_{\mathbf{k}}(\omega)=\sum_{ij}\Delta_{\mathbf{k}j}A_{ji}(\varepsilon_k-\omega)\Delta_{i\mathbf{k}}, \tag{3}$$

where $A(\omega)$ is the one-electron spectral function. The arguments leading to this expression do not say which one-electron states should be chosen for the photoelectron. This can only be decided by explicitly considering the left-out contribution in Eq. (2). Since the states $\mathbf{k}$ in Eq. (2) are not uniquely defined, the division between intrinsic and extrinsic contributions is somewhat arbitrary, except at high energies. In Appendix A we make a choice for this division.

The sudden approximation includes ''intrinsic losses'' or satellite structure, while the remaining term in Eq. (2) gives the ''extrinsic losses.'' Extrinsic and intrinsic losses thus *add amplitudes, not intensities* in the expression for the photocurrent in Eq. (1).

If we use an effective one-electron Hamiltonian h, and approximate the self-energy in A by an imaginary constant, $-i\Gamma$, then $A(\omega)=-\pi^{-1}\mathrm{Im}[\omega-h+i\Gamma]^{-1}$, and we have an approximation discussed in detail by, e.g., Feibelman and Eastman,[22] and by Pendry.[23] This approximation thus describes only the quasiparticle bands, and no satellite structures (intrinsic or extrinsic). There is no unique definition for h in Pendry's approach.

B. General discussion of core-electron photoemission using an electron-boson model Hamiltonian

The standard theory for photoemission uses the three-current formulation[2,3] expanding in Keldysh diagrams. Here we will instead follow a simple direct approach developed in Ref. 7, where we approximate the Hamiltonian by keeping only the simplest terms that give extrinsic losses,

$$H=H_s+h+V, \tag{4}$$

$$H_s=\sum_{\mathbf{q}}\omega_{\mathbf{q}}a_{\mathbf{q}}^\dagger a_{\mathbf{q}},\quad h=\sum_{\mathbf{k}}^{unocc}\epsilon_{\mathbf{k}}c_{\mathbf{k}}^\dagger c_{\mathbf{k}},$$

$$V=\sum_{\mathbf{qkk}'}V_{\mathbf{kk}'}^{\mathbf{q}}(a_{\mathbf{q}}+a_{\mathbf{q}}^\dagger)c_{\mathbf{k}}^\dagger c_{\mathbf{k}'};\quad V_{\mathbf{kk}'}^{\mathbf{q}}=\langle\mathbf{k}|V^{\mathbf{q}}(\mathbf{r})|\mathbf{k}'\rangle, \tag{5}$$

$$V^{\mathbf{q}}(\mathbf{r})=\int v(\mathbf{r}-\mathbf{r}')\langle\mathbf{q}|\rho(\mathbf{r}')|0\rangle d\mathbf{r}'. \tag{6}$$

Here H_s describes the solid with all the electron-electron interactions, h the photoelectron, and V the interaction between the photoelectron and the solid. H_s thus describes intrinsic losses, and V extrinsic losses, and also the damping of the photoelectron. The operators $a_{\mathbf{q}}^{\dagger}$ create exited states of the solid (quasibosons), with excitation energy $\omega_{\mathbf{q}}$, and the operators $c_{\mathbf{k}}^{\dagger}$ create photoelectrons in time-inverted LEED states with free-electron energies. $V^{\mathbf{q}}$ is a fluctuation potential, cf Eq. (50). For simplicity we use a single index $\mathbf{q}$ to design our bosons. We actually have both bulk and surface plasmons (which depend only on the momentum parallel to the surface), as well as (in the RPA case), electron-hole pairs, $c_{\mathbf{k}+\mathbf{q}}^{\dagger}c_{\mathbf{k}}$, depending on an additional index $\mathbf{k}$. For core-electron photoemission all quantities in H refer to the situation with one core hole present. A detailed motivation for this approximation can be made in the high-energy limit, see Appendix A.

The initial state has no photoelectrons, no quasibosons, and the core-electron state b is occupied. We write $|\Psi_i\rangle = b^{\dagger}|0'\rangle$. The ground state $|0'\rangle$ is for valence electrons with no core hole. $(H-E)$ in Eq. (2) can be replaced by V since $(H_s+h-E)c_k^{\dagger}|s\rangle=0$, and we can write the final state as

$$|\Psi_{\mathbf{k}s}\rangle=\left[1+\frac{1}{E-H-i\eta}V\right]c_{\mathbf{k}}^{\dagger}|s\rangle.$$

The state $|s\rangle$ contains $n_{\mathbf{q}}(s)$ quasibosons''$\mathbf{q}$.'' The photoelectron current becomes [cf. Eq. (1)]

$$J_{\mathbf{k}}(\omega)=\sum_s |\tau_s(\mathbf{k})|^2\delta\left(\omega-\varepsilon_{\mathbf{k}}-\sum_{\mathbf{q}} n_{\mathbf{q}}(s)\omega_{\mathbf{q}}\right), \qquad (7)$$

with the transition amplitude

$$\tau_s(\mathbf{k})=\left\langle s\left|c_{\mathbf{k}}\left[1+V\frac{1}{E-H+i\eta}\right]\sum_{ij}\Delta_{ij}c_i^{\dagger}c_j b^{\dagger}\right|0'\right\rangle. \qquad (8)$$

We have shifted the energy scale for ω to remove the large core-electron binding energy ϵ_c, such that the maximum energy that the photoelectron can have is ω. For the photoelectron we have put the energy zero at the bottom of the conduction band. When the photoelectron barely can leave the solid, and thus has zero kinetic energy, it is assigned the energy $\epsilon_F+\phi$, where ϵ_F is the Fermi energy, and ϕ the work function ($\phi>0$). The minimum possible value for ω is hence $\epsilon_F+\phi$.

In Eq. (8), c_j must annihilate the core electron, and $c_i^{\dagger}$ create a (virtual) photoelectron. Going over to a product space, we obtain

$$\tau_s(\mathbf{k})=\langle\mathbf{k}|\left\langle s\left|1+V\frac{1}{E-H+i\eta}\right|0'\right\rangle\sum_{\mathbf{k}'}|\mathbf{k}'\rangle\langle\mathbf{k}'|\Delta|c\rangle$$

$$\approx\langle\mathbf{k}|\left\langle s\left|1+V\frac{1}{E-H+i\eta}\right|0'\right\rangle\Delta|c\rangle, \qquad (9)$$

where, in the last line, we have approximated $\Sigma_{\mathbf{k}'}|\mathbf{k}'\rangle\langle\mathbf{k}'|$ by a δ function.

In Eq. (9), $|0'\rangle$ stands for the ground state of the valence electrons before the core electron was removed, while $|s\rangle$ stands for a state of the valence electrons in the presence of the core hole, and $|s=0\rangle=|\{n_{\mathbf{q}}=0\}\rangle$ is the completely relaxed state. The ground state $|0'\rangle$ is an eigenfunction of

$$H_s'=\sum_{\mathbf{q}}\omega_{\mathbf{q}}a_{\mathbf{q}}^{\dagger}a_{\mathbf{q}}+\sum_{\mathbf{q}}V_{cc}^{\mathbf{q}}(a_{\mathbf{q}}+a_{\mathbf{q}}^{\dagger}). \qquad (10)$$

To diagonalize H_s' we make a shift in the oscillators, $a_{\mathbf{q}}=\overline{a_{\mathbf{q}}}-V_{cc}^{\mathbf{q}}/\omega_{\mathbf{q}}$, and have

$$H_s'=\sum_{\mathbf{q}}\omega_{\mathbf{q}}\overline{a_{\mathbf{q}}^{\dagger}}\,\overline{a_{\mathbf{q}}}-\sum_{\mathbf{q}}\frac{(V_{cc}^{\mathbf{q}})^2}{\omega_{\mathbf{q}}}.$$

The second term is an energy shift, which we drop. The relation between the ground state $|0\rangle$ of $\Sigma_{\mathbf{q}}\omega_{\mathbf{q}}a_{\mathbf{q}}^{\dagger}a_{\mathbf{q}}$, and $|0'\rangle$ of $\Sigma_{\mathbf{q}}\omega_{\mathbf{q}}\overline{a_{\mathbf{q}}^{\dagger}}\,\overline{a_{\mathbf{q}}}$ is

$$|0'\rangle=e^{-S}|0\rangle, \quad S=\sum_{\mathbf{q}}\left[\frac{V_{cc}^{\mathbf{q}}}{\omega_{\mathbf{q}}}a_{\mathbf{q}}^{\dagger}+\frac{1}{2}\left(\frac{V_{cc}^{\mathbf{q}}}{\omega_{\mathbf{q}}}\right)^2\right]. \qquad (11)$$

We have for $\tau_s(\mathbf{k})$,

$$\tau_s(\mathbf{k})=\langle\mathbf{k}|\left\langle s\left|\left[1+V\frac{1}{E-H+i\eta}\right]e^{-S}\right|0\right\rangle\Delta|c\rangle \qquad (12)$$

We next make a partial summation in V to obtain damped photoelectron states. From Feshbach's projection operator techniques,[24] with $P+Q=1$, and $V=H_{PQ}+H_{QP}$, we have

$$P\left(1+V\frac{1}{E-H+i\eta}\right)=\frac{P(E-H_{PP}+i\eta)}{E-H_{PP}-\Sigma_{PP}+i\eta}\times\left(1+V_{PQ}\frac{1}{E-H_{QQ}+i\eta}\right),$$

$$\Sigma_{PP}=V_{PQ}[E-H_{QQ}+i\eta]^{-1}V_{QP}.$$

Choosing $P=|s\rangle\langle s|$, we have

$$H_{PP}=\left(\sum_{\mathbf{q}} n_{\mathbf{q}}(s)\omega_{\mathbf{q}}+h\right)P,$$

$$V_{PQ}=P\sum_{\mathbf{q}}(a_{\mathbf{q}}+a_{\mathbf{q}}^{\dagger})V^{\mathbf{q}}Q, \quad V_{QP}=Q\sum_{\mathbf{q}}\cdots P.$$

This gives

$$\tau_s(\mathbf{k})=\langle\tilde{\mathbf{k}}|\left\langle s\left|\left(1+V_{PQ}\frac{1}{E-H_{QQ}+i\eta}\right)e^{-S}\right|0\right\rangle\Delta|c\rangle, \qquad (13)$$

where $\langle\tilde{\mathbf{k}}|$ is a damped photoelectron state

$$\langle\tilde{\mathbf{k}}|=\langle\mathbf{k}|\frac{i\eta}{\epsilon_{\mathbf{k}}-h-\Sigma_{PP}+i\eta}.$$

To estimate Σ_{PP} we replace H_{QQ} by its lowest-order expression, H_s+h, which gives

$$\Sigma_{PP}(\epsilon_{\mathbf{k}})=\sum_{\mathbf{q}\mathbf{k}\mathbf{k}'\mathbf{k}''}\frac{V^{\mathbf{q}}_{\mathbf{k}\mathbf{k}''}V^{\mathbf{q}}_{\mathbf{k}''\mathbf{k}'}}{\epsilon_{\mathbf{k}}-\epsilon_{\mathbf{k}''}-\omega_{\mathbf{q}}+i\eta}c^{\dagger}_{\mathbf{k}}c_{\mathbf{k}'}.$$

The imaginary part of Σ_{PP} is precisely the polarization part in the GW approximation[18] for the self-energy, while the real part differs slightly. We note that in the present approximation Σ_{PP} does not depend on P, and we will hence omit the P index on Σ. In $\mathbf{r}$ space we have

$$\Sigma(\mathbf{r},\mathbf{r}';\omega)=\sum_{\mathbf{q}}V^{\mathbf{q}}(\mathbf{r})\frac{1}{\omega-h-\omega_{\mathbf{q}}+i\eta}V^{\mathbf{q}}(\mathbf{r}'). \quad (14)$$

We will now expand the transition amplitude to lowest nontrivial order in the fluctuation potentials when there are zero, one and two bosons excited. From S [cf. Eq. (11)] we have an overall prefactor, $e^{-a/2}$, where

$$a=\sum_{\mathbf{q}}\left(\frac{V^{\mathbf{q}}_{cc}}{\omega_{\mathbf{q}}}\right)^2. \quad (15)$$

We write

$$\tau_s(\mathbf{k})=e^{-a/2}\langle\tilde{\mathbf{k}}|T_s\Delta|c\rangle,$$

$$T_s=\left\langle s\left|\left(1+V\frac{Q}{E-H_{QQ}+i\eta}\right)e^{-\sum_{\mathbf{q}}(V^{\mathbf{q}}_{cc}/\omega_{\mathbf{q}})a^{\dagger}_{\mathbf{q}}}\right|0\right\rangle.$$

First consider a state s with one boson $\mathbf{q}_0$ excited, $n_{\mathbf{q}}(s)=\delta_{\mathbf{q},\mathbf{q}_0}$,

$$T_s=\left[\langle\mathbf{q}_0|V|0\rangle\left\langle 0\left|\frac{Q}{E-H_{QQ}+i\eta}\right|0\right\rangle-\frac{V^{\mathbf{q}_0}_{cc}}{\omega_{\mathbf{q}_0}}\right].$$

We further have (see Refs. 26,27),

$$\left\langle 0\left|\frac{Q}{E-H_{QQ}+i\eta}\right|0\right\rangle=G(\epsilon_{\mathbf{k}}+\omega_{\mathbf{q}_0}),$$

where

$$G(\omega)=\frac{1}{\omega-h-\Sigma(\omega)}$$

with Σ given in Eq. (14). Collecting our results we have

$$T_s=V^{q_0}G(\epsilon_{\mathbf{k}}+\omega_{\mathbf{q}_0})-\frac{V^{\mathbf{q}_0}_{cc}}{\omega_{\mathbf{q}_0}}, \quad (16)$$

where the first term gives extrinsic and the second intrinsic losses.

Next consider the case $n_{\mathbf{q}}(s)=0$, i.e., $|s\rangle=|0\rangle$,

$$T_s=1-\sum_{\mathbf{q}}V^{\mathbf{q}}G(\epsilon_{\mathbf{k}}-\omega_{\mathbf{q}})\frac{V^{\mathbf{q}}_{cc}}{\omega_{\mathbf{q}}}+\sum_{\mathbf{q}}V^{\mathbf{q}}G(\epsilon_{\mathbf{k}}-\omega_{\mathbf{q}})V^{\mathbf{q}}G(\epsilon_{\mathbf{k}}). \quad (17)$$

The last term was neglected in Ref. 7.

It is possible to develop a general expansion for $\tau_s(\mathbf{k})$. For the lowest-order contribution to two-boson excitations, [for example, $n_{\mathbf{q}_1}(s)=n_{\mathbf{q}_2}(s)=1$, all other $n_{\mathbf{q}}(s)=0$], we have

$$\begin{aligned}T_s=&\frac{V^{\mathbf{q}_1}_{cc}V^{\mathbf{q}_2}_{cc}}{\omega_{\mathbf{q}_1}\omega_{\mathbf{q}_2}}+\left(\frac{-V^{\mathbf{q}_1}_{cc}}{\omega_{\mathbf{q}_1}}\right)V^{\mathbf{q}_2}G(\varepsilon_{\mathbf{k}}+\omega_{\mathbf{q}_2})\\&+\left(\frac{-V^{\mathbf{q}_2}_{cc}}{\omega_{\mathbf{q}_2}}\right)V^{\mathbf{q}_1}G(\varepsilon_{\mathbf{k}}+\omega_{\mathbf{q}_1})++V^{\mathbf{q}_1}G(\varepsilon_{\mathbf{k}}+\omega_{\mathbf{q}_1})\\&\times V^{\mathbf{q}_2}G(\varepsilon_{\mathbf{k}}+\omega_{\mathbf{q}_1}+\omega_{\mathbf{q}_2})+V^{\mathbf{q}_2}G(\varepsilon_{\mathbf{k}}+\omega_{\mathbf{q}_2})\\&\times V^{\mathbf{q}_1}G(\varepsilon_{\mathbf{k}}+\omega_{\mathbf{q}_1}+\omega_{\mathbf{q}_2}). \quad (18)\end{aligned}$$

We will return to this two-boson expression in Sec. II D.

C. Detailed results for the one-boson satellites $[n_{\mathbf{q}}(s)=\delta_{\mathbf{q},\mathbf{q}_0}]$

1. General results in the semi-infinite jellium case

We want to evaluate approximations for $\tau_s(\mathbf{k})$ to obtain the photocurrent from Eq. (7). Since we have only one boson in the final states s, we will in this section for simplicity write $\tau_{\mathbf{q}}(\mathbf{k})$ instead of $\tau_s(\mathbf{k})$. We have

$$J_{\mathbf{k}}(\omega)=\sum_{\mathbf{q}}|\tau_{\mathbf{q}}(\mathbf{k})|^2\delta(\omega-\varepsilon_{\mathbf{k}}-\omega_{\mathbf{q}}). \quad (19)$$

We consider a half-infinite electron gas with an embedded ion at distance $z_c>0$ from the surface. We take the self-energy as zero outside the solid, and $-i\Gamma(\omega)$ inside. Neglecting the influence of the embedded ion, the fluctuation potential can be written

$$V^{\mathbf{q}}(\mathbf{r})=e^{i\mathbf{Q}\cdot\mathbf{R}}V^{\mathbf{q}}(z). \quad (20)$$

Bold capitals are used for vector components parallel to the surface, and small thin letters for the z components, $\mathbf{r}=(\mathbf{R},z)$, $\mathbf{k}=(\mathbf{K},k)$ and $\mathbf{q}=(\mathbf{Q},q)$, except that r means $|\mathbf{r}|$.

For the LEED state we write $(k>0)$,

$$|\tilde{\mathbf{k}},\mathrm{LEED}\rangle=e^{i\mathbf{K}\cdot\mathbf{R}}\{[e^{ikz}+Re^{-ikz}]\theta(-z)+Te^{i\tilde{k}z}\theta(z)\},$$

where

$$\tilde{k}=\sqrt{k^2+2[\phi\epsilon_F+\phi+i\Gamma(\epsilon_{\mathbf{k}})]}, \quad (21)$$

with ϕ the work function $(\phi>0)$. We set the transmission factor $T=1$, and correspondingly the reflection factor $R=0$, which is a good approximation except for very low energies, where in any case our approximations are less reliable. The photoelectron state is the time-inverted (i.e., complex conjugated, since we have no magnetic fields) LEED state. We have

$$|\tilde{\mathbf{k}}\rangle=e^{-i\mathbf{K}\mathbf{R}}[\theta(z)e^{-i\tilde{k}^*z}+\theta(-z)e^{-ikz}].$$

The intrinsic and extrinsic contributions to the transition amplitude become [cf. Eq. (16)]

$$\tau_{\mathbf{q}}^{intr}(\mathbf{k}) = -e^{-a/2}\langle \tilde{\mathbf{k}}|\Delta|c\rangle \frac{V_{cc}^{\mathbf{q}}}{\omega_{\mathbf{q}}}, \tag{22}$$

$$\langle \tilde{\mathbf{k}}|\Delta|c\rangle = e^{i\tilde{k}z_c}\langle \tilde{k}|\Delta|c\rangle^0, \tag{23}$$

$$\langle \tilde{k}|\Delta|c\rangle^0 = \int e^{i\tilde{k}(z-z_c)} e^{i\mathbf{K}\cdot\mathbf{R}} \Delta(z,\mathbf{R})\varphi_c(z,\mathbf{R})\,dz\,d\mathbf{R},$$

$$\tau_{\mathbf{q}}^{extr}(\mathbf{k}) = e^{-a/2}\int e^{i\tilde{k}z} V^{\mathbf{q}}(z) G(z,z';\kappa) e^{i(\mathbf{Q}+\mathbf{K})\cdot\mathbf{R}} \times \Delta(z',\mathbf{R})\varphi_c(z',\mathbf{R})\,dz\,dz'\,d\mathbf{R},$$

$$G(z,z';\kappa) = -\frac{i}{\kappa} e^{i\kappa|z-z'|},$$

$$\kappa = \sqrt{2[\omega+\phi+i\Gamma(\omega)] - |\mathbf{Q}+\mathbf{K}|^2}. \tag{24}$$

In κ we could replace $\epsilon_{\mathbf{k}}+\omega_{\mathbf{q}}$ by ω since we have an energy-conserving δ function in Eq. (19). Let us take the core-electron as centered at $(\mathbf{0},z_c)$, and neglect the $\mathbf{R}$ dependence in the exponents, since the core-electron wave function is strongly localized. We can also replace z' by z_c in $G(z,z';\kappa)$, and approximate $V_{cc}^{\mathbf{q}} = V^{\mathbf{q}}(z_c)$. We then have

$$\tau_{\mathbf{q}}^{intr}(\mathbf{k}) = -\langle \tilde{k}|\Delta|c\rangle^0 e^{i\tilde{k}z_c - a/2} \frac{V^{\mathbf{q}}(z_c)}{\omega - \epsilon_{\mathbf{k}}},$$

$$\tau_{\mathbf{q}}^{extr}(\mathbf{k}) = \langle \kappa|\Delta|c\rangle^0 e^{-a/2}\int e^{i\tilde{k}z} V^{\mathbf{q}}(z) G(z,z_c;\kappa)\,dz, \tag{25}$$

$$\langle k|\Delta|c\rangle^0 = \int e^{ik(z-z_c)}\Delta(z,\mathbf{R})\varphi_c(z,\mathbf{R})\,dz\,d\mathbf{R}.$$

The contributions to the integral giving $\langle k|\Delta|c\rangle^0$ come mainly from a small region close to $z=z_c$. In that region we should replace $e^{ik(z-z_c)}$ by a wave function that is forced by the strong ionic potential to have rapid oscillations. One finds, with an s core function, polarization in the z direction, and taking the origin of the photoelectron wave function at the ion core, $(\mathbf{0},z_c)$, that $\langle k|\Delta|c\rangle^0$ should be replaced by

$$\langle \mathbf{k}|\Delta|c\rangle = 4\pi i Y_{10}(\hat{\mathbf{k}})\Delta_c(|\mathbf{k}|),$$

$$\Delta_c(|\mathbf{k}|) = \int_0^\infty r^2 R_1(r;|\mathbf{k}|)\Delta(r)\phi_c(r)\,dr,$$

where R_1 is the radial solution of the atomic potential that matches smoothly to the p wave part of the plane wave. $\Delta_c(|\mathbf{k}|)$ varies only slowly with $|\mathbf{k}|$, while $\langle k|\Delta|c\rangle^0$ is proportional to k. At high enough energies the plane wave should be good, but then the approximation of neglecting the $e^{i\mathbf{KR}}$ factor is not valid. In the following we will put $\langle k|\Delta|c\rangle^0$ in Eq. (25) equal to 1, and thus disregard the angular function $|Y_{10}(\hat{\mathbf{k}})|^2$, which is a common factor for photoemission in a given direction, as well as the slowly varying function $\Delta_c(|\mathbf{k}|)$.

We have previously found[7] that contributions when the photoelectron travels *away* from the surface are very small, and neglect such contributions to G. The total transition amplitude then is,[25]

$$|\tau_{\mathbf{q}}(\mathbf{k})| = e^{-z_c Im\tilde{k} - a/2}|g_{\mathbf{q}}|, \tag{26}$$

$$g_{\mathbf{q}} = \left|\int_{-\infty}^{\infty} f(z) V^{\mathbf{q}}(z)\,dz\right|,$$

$$f(z) = \frac{\delta(z-z_c)}{\omega-\epsilon_{\mathbf{k}}} + \frac{i}{\kappa} e^{i(\tilde{k}-\kappa)(z-z_c)}\theta(z_c-z),$$

$$g_{\mathbf{q}} = \left|\frac{V^{\mathbf{q}}(z_c)}{\omega-\epsilon_{\mathbf{k}}} + \frac{i}{\kappa}\int_{-\infty}^{z_c} e^{i(\tilde{k}-\kappa)(z-z_c)} V^{\mathbf{q}}(z)\,dz\right|. \tag{27}$$

Since $J_{\mathbf{k}}(\omega)$ is quadratic in the fluctuation potentials, we can write the photocurrent in terms of the imaginary part of the screened interaction. From Eq. (B3) we have for the parallel momentum Fourier transform of $\mathrm{Im}\,W(\mathbf{r},\mathbf{r}';\omega)$ [cf. also Eq. (20)],

$$\mathrm{Im}W(\mathbf{Q},z,z';\omega) = -\pi A\sum_q V^{\mathbf{q}}(z)V^{\mathbf{q}}(z')^*\delta(\omega-\omega_{\mathbf{q}}), \tag{28}$$

where the asterisk means complex conjugate, and A is the normalization area, the normalization volume being $\Omega = AL$. Taking the core-electron wave function as having zero extent, we obtain from Eqs. (19) and (26),

$$J_{\mathbf{k}}(\omega) = e^{-2z_c \mathrm{Im}\,\tilde{k} - a}\sum_{\mathbf{q}} |g_{\mathbf{q}}|^2 \delta(\omega-\varepsilon_{\mathbf{k}}-\omega_{\mathbf{q}}). \tag{29}$$

Comparison with Eq. (28) gives,

$$J_{\mathbf{k}}(\omega) = e^{-2z_c \mathrm{Im}\,\tilde{k} - a}\frac{-1}{\pi A}\sum_{\mathbf{Q}} \int f(z)f(z')^* \times \mathrm{Im}\,W(\mathbf{Q},z,z';\omega-\varepsilon_{\mathbf{k}})\,dz\,dz'. \tag{30}$$

The first (intrinsic) term in $f(z)$ will clearly dominate close to threshold, $\omega=\varepsilon_{\mathbf{k}}$.

2. Explicit results with the Inglesfield bulk fluctuation potential

The Inglesfield bulk plasmon potential is (in atomic units)

$$V^{\mathbf{q}}(z) = A_{\mathbf{q}}[\cos(qz+\phi_{\mathbf{q}}) - \cos\phi_{\mathbf{q}} e^{-Qz}]\theta(z), \tag{31}$$

$$A_{\mathbf{q}} = \sqrt{\frac{4\pi\omega_p^2}{\Omega(Q^2+q^2)\omega_{\mathbf{q}}}}, \quad \phi_{\mathbf{q}} = \mathrm{arctg}\frac{Q}{q},$$

$$\omega_{\mathbf{q}} = \omega_p + \tfrac{1}{2}(Q^2+q^2).$$

Using Eq. (27), we have the simple expression

$$g_{\mathbf{q}}=A_{\mathbf{q}}e^{i(\kappa-\tilde{k})z_c}\left\{\frac{e^{i\phi_{\mathbf{q}}}R(\tilde{k}-\kappa+q)}{2\kappa}+\frac{e^{-i\phi_{\mathbf{q}}}R(\tilde{k}-\kappa-q)}{2\kappa}\right.$$
$$\left.-\frac{\cos\phi_{\mathbf{q}}R(\tilde{k}-\kappa+iQ)}{\kappa}-\frac{\cos(qz_c+\phi_{\mathbf{q}})-\cos\phi_{\mathbf{q}}e^{-Qz_c}}{\omega_{\mathbf{q}}}\right\}, \tag{32}$$

where $R(x)=(1-e^{ixz_c})/x$.

We see that the damping is proportional to z_c, whereas we should expect it to be proportional to the length $l=z_c/\cos\varphi$ traveled by the electron coming out at an angle φ to the normal. The combination $z_c\mathrm{Im}\,\tilde{k}$, however, has the expected behavior, at least at high energy. From Eq. (21) we have

$$2z_c\mathrm{Im}\tilde{k}\cong\frac{2\Gamma z_c}{k}\cong\frac{2\Gamma l\cos\varphi}{|\mathbf{k}|\cos\varphi}=\frac{l}{\lambda}, \tag{33}$$

where λ is the mean field path, $v/(2\Gamma)$.

For photoemission at right angle to the surface, $\mathbf{K}=0$, the $\mathbf{K}\cdot\mathbf{Q}$ term in κ disappears, and we are left with only one integral in Eq. (29), which then becomes

$$J_{\mathbf{k}}(\omega)=\frac{e^{-2z_c\mathrm{Im}\tilde{k}-a}\omega_p^2\theta(q_0)}{\pi q_0^2(\omega-\varepsilon_{\mathbf{k}})}\int_{-q_0}^{q_0}\left|\frac{g_{\mathbf{q}}}{A_{\mathbf{q}}}\right|^2_{Q=\sqrt{q_0^2-q^2}}dq, \tag{34}$$

$$q_0=\sqrt{2(\omega-\omega_p-\varepsilon_{\mathbf{k}})}.$$

3. High-energy and large-z_c limit

We want to evaluate $J_{\mathbf{k}}(\omega)$ in the limit of high energy and large z_c, and show that we obtain the same result as in the Berglund-Spicer model. For large energies

$$\kappa\cong\tilde{k}\cong k,\ \mathrm{Re}(\kappa-\tilde{k})\cong\frac{\omega_p+q^2/2}{k},$$

$$\mathrm{Im}(\kappa-\tilde{k})\cong\frac{\Gamma(\omega)-\Gamma(\omega-\omega_{q_0})}{k}.$$

$\Gamma(\omega)$ starts quadratically at the Fermi surface, increases rapidly at the onset of plasmon decay at about $\epsilon_F+(1+0.24\sqrt{r_s})\omega_p$, reaches a broad maximum slightly below $\epsilon_F+3\omega_p$, and then slowly goes to zero as $1/\sqrt{\omega}$. From this it follows that in the high-energy limit, we can neglect $\mathrm{Im}(\kappa-\tilde{k})$ which appears as a prefactor in the expression for $g_{\mathbf{q}}$ in Eq. (27). Neglecting the cross terms (interference terms) in $|g_{\mathbf{q}}|^2$ we have

$$\left|\frac{g_{\mathbf{q}}}{A_{\mathbf{q}}}\right|^2=\frac{1}{4k^2}\{|R(\tilde{k}-\kappa+q)|^2+|R(\tilde{k}-\kappa-q)|^2\}$$
$$+\frac{\cos^2(qz_c+\phi_{\mathbf{q}})}{\omega_{\mathbf{q}}^2}.$$

We have dropped the $\cos\phi_{\mathbf{q}}R(\tilde{k}-\kappa+iQ)$ term, since for large energies the result cannot depend on the phase shift $\phi_{\mathbf{q}}$ at the surface. One can also explicitly verify that this term is much smaller than those that we have kept. We have also dropped the $\cos\phi_{\mathbf{q}}e^{-Qz_c}$ term, which vanishes for large z_c. For large z_c, $\cos^2(qz_c+\phi_{\mathbf{q}})$ averages to 1/2. Further $|R(x)|^2=[4\sin^2(xz_c/2)]x^2\cong 2\pi z_c\delta(x)$, and thus

$$J_{\mathbf{k}}(\omega)=\frac{e^{-2z_c\mathrm{Im}\,\tilde{k}-a}\omega_p^2\theta(q_0)}{\pi q_0^2(\omega-\varepsilon_k)}\left[\frac{\pi z_c}{k^2}+\frac{q_0}{(\omega-\varepsilon_k)^2}\right]. \tag{35}$$

D. Generalization of Eq. (29) to an exponential form

We can write an exponential expression that in lowest order reproduces Eq. (29), and picks up the most divergent terms in higher order in the expansion made in Sec. II B,

$$J_{\mathbf{k}}(\omega)=\frac{1}{2\pi}\int_{-\infty}^{\infty}e^{i(\omega-\varepsilon_k)t}e^{\Sigma_{\mathbf{q}}|g_{\mathbf{q}}|^2(e^{-i\omega_{\mathbf{q}}t}-1)}dt, \tag{36}$$

First we expand Eq. (36) as

$$J_{\mathbf{k}}(\omega)=e^{-\Sigma_{\mathbf{q}}|g_{\mathbf{q}}|^2}\left[\delta(\omega-\varepsilon_k)+\sum_{\mathbf{q}}|g_{\mathbf{q}}|^2\delta(\omega-\varepsilon_k-\omega_{\mathbf{q}})\right]. \tag{37}$$

This is meaningful only when the $\omega_{\mathbf{q}}$ have a positive minimum value, i.e., when the particle-hole continuum is omitted, since otherwise $g_{\mathbf{q}}$ diverges when $\omega=\epsilon_{\mathbf{k}}$, cf. Eq. (27). The exponential expression, on the other hand, is well defined also with the particle-hole terms included. The δ function in Eq. (37) gives the quasiparticle contribution, and the second term reproduces Eq. (29) provided

$$\sum_{\mathbf{q}}|g_{\mathbf{q}}|^2=a+2z_c\mathrm{Im}\,\tilde{k}. \tag{38}$$

In the high-energy limit we have from Eqs. (35) and (37),

$$\sum_{\mathbf{q}}|g_{\mathbf{q}}|^2=\int d\omega\left[\frac{\omega_p^2\theta(q_0)}{\pi q_0^2(\omega-\varepsilon_k)}\left(\frac{\pi z_c}{k^2}+\frac{q_0}{(\omega-\varepsilon_k)^2}\right)\right]. \tag{39}$$

The second term in Eq. (39) comes from the intrinsic contribution,

$$\frac{\omega_p^2\theta(\omega-\omega_p)}{\pi\omega^3\sqrt{2(\omega-\omega_p)}}=\frac{\alpha(\omega)}{\omega}, \tag{40}$$

where $\alpha(\omega)$ is the Langreth singularity function, defined so that $\alpha(0)$ is the singularity index for the core-electron spectral line, $A_c(\omega)\approx\omega^{-[1-\alpha(0)]}$ (cf. p. 655 in Ref. 28). The first term in Eq. (39) is related to what Ritchie[31] calls the DIMFP function $\tau(\epsilon,\omega)$ (differential inverse mean free path, see e.g., p. 689 in Ref. 28), where ϵ is the photoelectron energy,

$$\tau(\varepsilon,\omega)=\frac{1}{\pi\varepsilon}\int\frac{dq}{q}\mathrm{Im}\left[\frac{-1}{\epsilon(q,\omega)}\right].$$

Neglecting the weak (at higher energies) dependence on the electron energy ϵ, we have

$$\frac{\omega_p^2\theta(\omega-\omega_p)}{2(\omega-\omega_p)\omega\varepsilon}=\tau(\varepsilon,\omega).$$

The integral over $\alpha(\omega)/\omega$ gives the overlap factor a in Eq. (15), and over $\tau(\varepsilon,\omega)$ the inverse mean free path $\tau_0(\varepsilon)=1/\lambda$, cf. Eq. (33),

$$a=\int\frac{\alpha(\omega)}{\omega}d\omega,\quad \tau_0(\varepsilon)=\int\tau(\varepsilon,\omega)d\omega. \tag{41}$$

Thus Eq. (38) is correct at least in the high-energy limit. An example of the magnitude of the breakdown of Eq. (38) is given in Fig. 8.

We now turn to the higher-order terms in Eq. (36). It is easy to see that if we neglect the extrinsic losses, we arrive at the usual intrinsic spectrum with its asymmetric main line and all its satellite peaks. At threshold the intrinsic terms dominate, due to the factor $\omega-\epsilon_{\mathbf{k}}$ in the denominator [cf. Eq. (27)]. From the general expressions for expanding T_s (cf. Sec. II B), the next most singular term at threshold [cf. Eq. (18)] is exactly reproduced by the exponential expression to all orders, and for all energies. As regards the second-order term, it is reproduced exactly by Eq. (18) in the high-energy limit.

E. The Berglund-Spicer expression

The Berglund-Spicer approximation for the energy distribution $D(\omega,z)$ of the electron after it has traveled a distance z is

$$D(\omega,z)=\int A_c(\omega')P(\omega'-\omega;z)d\omega',$$

where $A_c(\omega)$ is the intrinsic spectrum given by the one-electron spectral function, and $P(\omega;z)$ is the probability that the electron has lost an energy ω when it has traveled a distance z. As shown in Ref. 28, $D(\omega,z)$ can be written in a compact form if we use results by Langreth[29] and Landau,[30]

$$D(\omega,z)=\int_{-\infty}^{\infty}\frac{e^{i\omega t}dt}{2\pi}\exp\left\{\int(d\omega'/\omega')\times[\alpha(\omega')+z\omega'\tau(\epsilon,\omega')](e^{-i\omega' t}-1)\right\}. \tag{42}$$

The dependence of $\tau(\epsilon,\omega)$ on ϵ is weak at high energies, and was neglected in Landau's derivation of $P(\omega)$. Neglecting the electron-hole contributions, so that $\alpha(\omega)$ and $\tau(\varepsilon,\omega)$ start at the plasmon loss threshold, we have

$$D(\omega,z)=e^{-a-\tau_0(\varepsilon)z}\left[\delta(\omega)+\frac{\alpha(\omega)}{\omega}+\tau(\varepsilon,\omega)z+\cdots\right]. \tag{43}$$

When we evaluate $\tau_0(\varepsilon)$, $\alpha(\omega)$, and $\tau(\varepsilon,\omega)$ in the plasmon-pole approximation, the satellite part in Eq. (43) precisely reproduces Eq. (35).

When we integrate $D(\omega,z)$ over z, we have the well-known result[32]

$$\int D(\omega,z)dz=\frac{e^{-a}}{\tau_0(\varepsilon)}\left[\delta(\omega)+\frac{\alpha(\omega)}{\omega}+\frac{\tau(\varepsilon,\omega)}{\tau_0(\varepsilon)}+\cdots\right].$$

If we also integrate over ω we obtain,

$$\int D(\omega,z)dzd\omega=\frac{e^{-a}}{\tau_0(\varepsilon)}[1+a+1+\cdots]. \tag{44}$$

The relative intensity of the first plasmon satellite to that of the main peak is thus always $a+1$ in the BS approximation. In our model calculations $a=0.35$.

As noted in Ref. 32 $\tau(\varepsilon,\omega)$ and $\tau_0(\varepsilon)$ tend to zero with increasing photoelectron energy ε. When we integrate Eq. (43) over z, we, however, cover a larger and larger distance, since $\tau_0(\varepsilon)$ in the exponent becomes smaller and smaller, and the total contribution from the extrinsic losses is always the same as in the elastic peak. If we have photoemission from a finite system, or from atoms on a surface, the distance the photoelectron travels is finite, and the extrinsic contributions vanish as the photoelectron energy increases.

F. Loss spectra from time-dependent perturbation theory

A simple approach to calculate loss spectra at high energies is to consider the effect of a classical particle moving on a trajectory. We then have a perturbation from a charge moving with velocity v. For simplicity we here assume that it moves at right angle towards the surface,

$$\rho(\mathbf{r},t)=[\delta(z+vt-z_c)-\delta(z-z_c)]\delta(\mathbf{R})\theta(t). \tag{45}$$

To describe the effect of the perturbation we can use the ''forced oscillator'' Hamiltonian,[15,33]

$$H(t)=\sum_{\mathbf{q}}[\omega_{\mathbf{q}}a_{\mathbf{q}}^{\dagger}a_{\mathbf{q}}+V_{\mathbf{q}}(t)(a_{\mathbf{q}}+a_{\mathbf{q}}^{\dagger})], \tag{46}$$

$$V_{\mathbf{q}}(t)=\int V^{\mathbf{q}}(\mathbf{r})\rho(\mathbf{r},t)d\mathbf{r}. \tag{47}$$

Here $V^{\mathbf{q}}(\mathbf{r})$ is the same fluctuation potential as we introduced in Eqs. (6) and (20). In Appendix C we calculate the probability $P(\varepsilon)$ that the time-dependent perturbation in $H(t)$ after a long time has excited the system with an energy ε. We then assume that $P(\varepsilon)$ also is the probability that the photoelectron has lost an energy ε, $J_{\mathbf{k}}(\omega)=P(\varepsilon)=P(\omega-\varepsilon_{\mathbf{k}})$. From Eq. (C2) in Appendix C we have

$$J_{\mathbf{k}}(\omega)=\frac{1}{2\pi}\int_{-\infty}^{\infty}e^{i(\omega-\varepsilon_k)t}e\sum_{\mathbf{q}}|g_{\mathbf{q}}^0|^2(e^{-i\omega_{\mathbf{q}}t}-1)dt.$$

The coupling function is obtained from Eqs. (45) and (47),

$$|g_{\mathbf{q}}^0|\equiv\left|\int_0^{\infty}e^{i\omega_{\mathbf{q}}t}V_{\mathbf{q}}(t)dt\right|=\left|\frac{i}{v}\int_{-\infty}^{z_c}dzV^{\mathbf{q}}(z)e^{-i\omega_{\mathbf{q}}(z-z_c)/v}+\frac{V^{\mathbf{q}}(z_c)}{\omega_{\mathbf{q}}}\right|.$$

We can compare $g_{\mathbf{q}}^0$ with $g_{\mathbf{q}}$ in Eq. (27). In our units $\mathbf{v}=\mathbf{k}$. At high energies $\tilde{k}\cong\kappa\cong k$, and $\tilde{k}-\kappa\cong-[(\omega_{\mathbf{q}}-Q^2/2)/k]$.

The semiclassical approach thus agrees with the quantum-mechanical one at high energies, as expected, and as has been noted before.[6,7] Here however we have gone one step further and obtained the exact solution to the semiclassical problem. This exponential expression for the solution is very similar to what we had in the Berglund-Spicer approach, and to what we postulated also for the quantum-mechanical case, Eq. (36). The lowest-order term in the quantum-mechanical and classical cases agree quite well already at the order of a plasmon energy above threshold. This gives further indications for the validity of Eq. (36).

G. The Tougaard approach

In the work of Simonsen, Yubero, and Tougaard[16] on photo-emission one finds a different formulation of the energy-loss process in terms of an induced potential. The medium is polarized by the sudden creation of core hole and photoelectron, and the resulting polarization charge acts on the moving electron. In this classical picture the outgoing electrons are decelerated by the induced potential field (ϕ_{ind}). The induced potential is found from a theory developed by Garcia-Moliner and Rubio (see, e.g., Ref. 17). The vacuum and medium parts of ϕ_{ind} are calculated separately, introducing pseudosurface charges at the interface to account for the removal of the other subsystem (e.g., the vacuum induced potential is calculated for a vacuum medium in all space, where the effect of removing the solid is counteracted by some pseudosurface charge). The pseudo-charges are found from the appropriate boundary conditions at the interface. In this method, as in Bechstedt's, the dielectric response can be easily formulated in terms of the bulk dielectric function, and also here the interference effects are not included. As a further approximation Tougaard uses a plasmon-pole model for the bulk dielectric function, combined with the assumption that the k_z dependence of $\epsilon(\mathbf{k},\omega)$ can be neglected in calculating the photoemission. Thus we should have, with $W_p = W - v$,

$$\begin{aligned}\int dz' W_p(\mathbf{Q},z,z',\omega)\rho_{ext}(\mathbf{Q},z',\omega) &= \theta(-z)\int \frac{dk_z}{2\pi} e^{-ik_z z}\phi^V_{ind}(\mathbf{k},\omega) \\ &+ \theta(z)\int \frac{dk_z}{2\pi} e^{-ik_z z}\phi^M_{ind}(\mathbf{k},\omega),\end{aligned} \tag{48}$$

where $\rho_{ext}(\mathbf{Q},z',\omega)$ is the two-dimensional Fourier transform of the core hole and photoelectron charge densities, while $\varphi^M_{ind}(\mathbf{k},\omega)$ and $\varphi^V_{ind}(\mathbf{k},\omega)$ are the full Fourier transforms of the induced potentials of the two subsystems (medium and vacuum). For their definition see Ref. 16. We have checked this relation explicitly by taking the screened interaction of Bechstedt, Enderlein, and Reichardt for W with the same approximations for $\epsilon(\mathbf{k},\omega)$ as used by Simonsen, Yubero, and Tougaard.

The approximation $\epsilon(\mathbf{k},\omega) = \epsilon(\mathbf{Q},\omega)$, however, implies the existence of *localized* bulk plasmon fluctuation potentials. For a description of the collective modes of the system, it is therefore inappropriate. Nevertheless the satellites obtained by Tougaard are similar to ours, but there are substantial quantitative differences, as we will discuss in Sec. IV.

III. FLUCTUATION POTENTIALS

A. General considerations

The exact formal expression for the dynamically screened interaction $W(\mathbf{r},\mathbf{r}';\omega)$ can be written as a spectral resolution,

$$W(\mathbf{r},\mathbf{r}';\omega) = v(\mathbf{r}-\mathbf{r}') + \sum_t \frac{2\omega_t V^t(\mathbf{r})V^t(\mathbf{r}')}{\omega^2-\omega_t^2}, \tag{49}$$

where $v(\mathbf{r}-\mathbf{r}')$ is the bare Coulomb potential, $v(\mathbf{r}-\mathbf{r}') = e^2/|\mathbf{r}-\mathbf{r}'|$, and $V^t(\mathbf{r})$ is the fluctuation potential,

$$V^t(\mathbf{r}) = \int v(\mathbf{r}-\mathbf{r}')\langle t|\rho(\mathbf{r}')|0\rangle d\mathbf{r}'. \tag{50}$$

We have expressed our theory for photoemission in terms of the fluctuation potentials $V^t(\mathbf{r})$. We noted that the photoelectron current, to lowest nontrivial order, is quadratic in the fluctuation potentials, Eq. (30), and can be described by $\mathrm{Im}\, W$. Still, it is useful to work directly with the fluctuation potentials, rather than with $\mathrm{Im}\, W$, since it allows a larger flexibility and more insight in developing approximations.

To obtain an approximation for $V^t(\mathbf{r})$ we write the RPA expression for W on the same spectral form as in Eq. (49). In RPA we have $W = (1-vP)^{-1}v$, with

$$P(\mathbf{r},\mathbf{r}';\omega) = \sum_t \frac{2\omega_t \varphi_t(\mathbf{r})\varphi_t^*(\mathbf{r}')}{\omega^2-\omega_t^2}. \tag{51}$$

Here $\varphi_t(\mathbf{r})$ is a particle-hole wave function, $\varphi_t(\mathbf{r}) = \psi_i(\mathbf{r})\psi_j^*(\mathbf{r})$, and $\omega_t = \varepsilon_i - \varepsilon_j (\varepsilon_i \geqslant \varepsilon_F \geqslant \varepsilon_j)$ a particle-hole energy. The index t stands for the pair (i,j). In Appendix B we have shown that we can use the real and imaginary parts of

$$V^t(\mathbf{r}) = \int W(\mathbf{r},\mathbf{r}';\omega_t)\varphi_t(\mathbf{r}')d\mathbf{r}' \tag{52}$$

in Eq. (49). We can easily check that this expression is correct to lowest nontrivial order in v. Replacing W by v in Eq. (52) we reproduce the Hartree-Fock approximation for Eq. (50), since in Hartree Fock

$$\langle N,t|\rho(\mathbf{r})|N\rangle = \sum_{ij} \psi_i^*(\mathbf{r})\psi_j(\mathbf{r})\langle N,t|c_i^\dagger c_j|N\rangle = \psi_i^*(\mathbf{r})\psi_j(\mathbf{r}),$$

with $t=(ij)$. If we expand $W=(1-vP)^{-1}v$ to second order in v, and use Eq. (51), we also reproduce Eq. (49) to second order.

In addition to the fluctuation potentials in Eq. (52) we can also have contributions to Eq. (49) from fluctuation potentials coming from solutions w_i to an eigenvalue problem, Eq. (B6) in Appendix B,

$$V^i(\mathbf{r}) = \left[\frac{\partial\lambda_i(\omega)}{\partial\omega}\right]^{-(1/2)}_{\omega=\omega_i} w_i(\mathbf{r},\omega_i). \tag{53}$$

Such solutions contribute only if ω_i is real [ω_i comes from $\lambda_i(\omega_i)=0$, cf. Eq. (B6)]. If ω_i is not real, the eigenmodes no longer correspond to undamped collective excitations of the system. If the imaginary part of ω_i is small, a mode $w_i(\mathbf{r},\omega_i)$ is however a useful approximation to a set of modes of the type in Eq. (52).

As another illustration of the nature of fluctuation potentials, consider an electron gas. Here we have contributions both from particle-hole pairs, $V^t(\mathbf{r})$ $(t=\mathbf{k},\mathbf{k}+\mathbf{q})$, and from plasmons, $V^{\mathbf{q}}(\mathbf{r})$,

$$V^t(\mathbf{r})=\left|\frac{v(|\mathbf{q}|)}{\epsilon(|\mathbf{q}|,\epsilon_{\mathbf{k}+\mathbf{q}}-\epsilon_{\mathbf{k}})}\right|e^{i\mathbf{q}\cdot\mathbf{r}},$$

$$V^{\mathbf{q}}(\mathbf{r})=\left|\frac{v(|\mathbf{q}|)}{\partial\epsilon(|\mathbf{q}|,\omega)/\partial\omega}\right|^{1/2}_{\omega=\omega_{\mathbf{q}}}e^{i\mathbf{q}\cdot\mathbf{r}}.$$

We can also write Eq. (49) in terms of the normalized eigenpotentials $w_i(\mathbf{r},\omega)$ (see Appendix B),

$$W(\mathbf{r},\mathbf{r}';\omega)=\sum_i\frac{w_i(\mathbf{r},\omega)w_i(\mathbf{r}',\omega)}{\lambda_i(\omega)}. \tag{54}$$

In this case we do not have to combine contributions $V^t(\mathbf{r})$ and $V^{\mathbf{q}}(\mathbf{r})$; however, the approach has the drawback that we need a different potential $w_i(\mathbf{r},\omega)$ for each ω, while in the earlier approach the energy ω_i in $w_i(\mathbf{r},\omega_i)$ was coupled to the state i.

It is useful to study simple analytic forms of the fluctuation potentials that illustrate the physics of the interaction between photoelectron and valence-electron systems, and in the next sections we introduce two simple forms and compare them with RPA results.

B. Inglesfield's fluctuation potentials

The Inglesfield bulk potential is given in Eq. (31), while his surface potential is just $N_s e^{-Q|z|}$. The arguments behind the Inglesfield potentials are the following.

It can be shown[10] that the bulk modes in a semi-infinite system are standing waves, i.e., phase-shifted cosines modified at the surface. The shape of the bulk modes at the surface and the magnitude of the phase shift are determined by the details of the surface dielectric response. In Ref. 6 Inglesfield assumed that the cosine form for the charge fluctuations was valid all the way to the surface; the phase shift was determined by assuming that the corresponding fluctuation potentials were zero at the surface. We obtain the required orthogonality of the bulk potential to the charge density of the surface modes (at the same frequency), if the surface charge fluctuations are assumed to be δ functions centered at $z=0$. The actual bulk fluctuation potentials are nonzero at the surface, as seen in Eq. (60), but the tails are quite small.

C. Fluctuation potentials from Bechstedt's model

Semiinfinite jellium, an electron gas confined by an infinite potential barrier, is a much used model.[8] If the interference terms in the polarization are neglected, we have a very simple expression for the polarization,

$$P(Q,z,z',\omega)=\theta(z)\,\theta(z')[P_o(Q,z-z',\omega)+P_o(Q,z+z',\omega)], \tag{55}$$

where Q is the magnitude of the two-dimensional momentum parallel to the surface, z and z' are coordinates perpendicular to the surface, and P_0 is the polarization function for the homogeneous electron gas. In this way the dielectric response of the semijellium problem is related to the response of the homogeneous bulk system. This approximation satisfies the f-sum rule.

Bechstedt, Enderlein, and Reichardt[9] were able to obtain a closed expression for the screened potential W corresponding to Eq. (55),

$$\begin{aligned}W(Q,z,z',\omega)=\frac{2\pi e^2}{Q}\{&\theta(-z)\,\theta(-z')\\&\times[e^{-Q|z-z'|}+(1-t_1)e^{Q(z+z')}]\\&+t_1[\theta(-z)\,\theta(z')a(Q,z',\omega)e^{Qz}\\&+\theta(z)\,\theta(-z')a(Q,z,\omega)e^{Qz'}]+\theta(z)\,\theta(z')\\&\times[a(Q,z-z',\omega)+a(Q,z+z',\omega)\\&-t_1a(Q,z,\omega)a(Q,z',\omega)]\},\end{aligned} \tag{56}$$

where $t_1=2[1+a(Q,0,\omega)]^{-1}$, and where $a(Q,z,\omega)$ is related to the bulk dielectric function $\epsilon_o(q,\omega)$

$$a(Q,z,\omega)=\frac{Q}{\pi}\int dq_z\frac{e^{iq_zz}}{|\mathbf{q}|^2\epsilon_o(|\mathbf{q}|,\omega)}. \tag{57}$$

For $\epsilon_o(|\mathbf{q}|,\omega)$ we use a simple plasmon-pole model

$$\frac{1}{\epsilon_o(|\mathbf{q}|,\omega)}=1+\frac{\omega_p^2}{\omega^2-\omega_{|\mathbf{q}|}^2}, \tag{58}$$

where $\omega_{|\mathbf{q}|}=\omega_p+\frac{1}{2}(q^2+Q^2)$ is the plasmon frequency. The quantity $a(Q,z,\omega)$ then assumes a simple analytic form and from the imaginary part of $W(Q,z,z',\omega)$ the fluctuation potentials can be extracted. For the surface fluctuation potentials we find

$$V^s(z,\omega)=N_s[\theta(-z)e^{Qz}+\theta(z)a(Q,z,\omega)] \tag{59}$$

and for the bulk fluctuation potentials,

$$\begin{aligned}V^b(z,\omega)=N_b[&\theta(-z)e^{Qz}+\theta(z)\{(2+C_1+C_3)\cos(qz)\\&+C_2\sin(qz)-(1+C_1)e^{-Qz}-C_3e^{-\sqrt{\omega+\omega_p+Q^2}z}\},\end{aligned} \tag{60}$$

where

$$C_1=\frac{\omega_p^2}{\omega^2-\omega_p^2},\quad C_2=\frac{-Q\omega_p^2}{2\omega(\omega-\omega_p)q},$$

$$C_3=\frac{-Q\omega_p^2}{2\omega(\omega+\omega_p)\sqrt{\omega+\omega_p+Q^2}}.$$

The N_s and N_b include coefficients due to normalization and coupling strength $|\partial\lambda_i(\omega)/\partial\omega|^{-(1/2)}_{\omega=\omega_i}$ (see Appendix B).

D. RPA fluctuation potentials and screened interaction

To calculate the RPA fluctuation potentials w_i it is convenient first to find the charge fluctuations $\delta\rho_i$, Eq. (B8). In our case with a semi-infinite jellium, the noninteracting Green's function has a simple form

$$G_o(Q,\omega;z,z')=\frac{e^{-\gamma|z-z'|}}{\gamma}\theta(z)\theta(z'), \tag{61}$$

$$\gamma=(Q^2-2\omega)^{1/2}\theta(Q^2-2\omega)-i(2\omega-Q^2)^{1/2}\theta(2\omega-Q^2),$$

from which the RPA polarization P can be calculated.[10] Equation (B8) can be Fourier transformed with respect to **R**, and then cosine transformed with respect to the z and z' coordinates. The resulting k_z integral is replaced by a discrete sum, see, e.g., Ref. 10. The modes with $\lambda_i(\omega)=0$ for real ω correspond to collective excitations of the system. Within the RPA only the bulk plasmon excitations are undamped. The surface modes satisfy $\lambda_i(\omega)=0$ for (slightly) complex frequencies and are damped complex modes. Outside the Landau damping region ($Q<Q_c=$ the Landau wave vector), it is a good approximation to neglect the imaginary parts. Indeed, the agreement between the RPA, and the Inglesfield and the Bechstedt surface fluctuation potentials is very good. The potentials are both roughly of the form $e^{-Q|z-z_0|}$ and the modes show very similar dispersion relations. Here z_0 is some small distance from the surface into the bulk (say, 2 a.u.) and depends only weakly on Q.

IV. RESULTS

We study a simple model, semi-infinite jellium with one atom at a distance z_c from the surface, and are interested in general trends when we go from threshold excitation to high energies. The final states are plane waves outside the solid. Inside the solid the waves are damped with an energy-dependent self-energy $\Gamma(\omega)$, calculated within the GW approximation for a homogeneous jellium (with the full RPA dielectric function). No surface emission, i.e., contribution from the gradient of the surface barrier, is considered. All calculations are for an electron density corresponding to Al, with $r_s=2.0724$. At this density the bulk plasmon energy $\omega_p=0.581$ a.u., the surface plasmon energy $\omega_p/\sqrt{2}=0.411$ a.u., and the Fermi energy $\varepsilon_F=0.429$ a.u. For the work-function we taken $\phi=0.147$ a.u. ($=4$ eV). For the Bechstedt and Inglesfield potentials we used a simple plasmon pole dielectric function [cf. Eq. (58)], which gives for the overlap factor a [cf. Eqs. (11,15)] $a=0.3480$. For the RPA calculations (which include particle-hole excitations) a semi-infinite jellium with an infinite potential at the boundary was used.

The RPA collective excitations (both bulk and surface) were calculated solving the eigenvalue equation (B8). The results agree very well with those from Bechstedt's model, especially at frequencies where Landau damping is not effective, and the surface modes thus couple weakly to the electron-hole pairs. As a specific example we show in Fig. 1

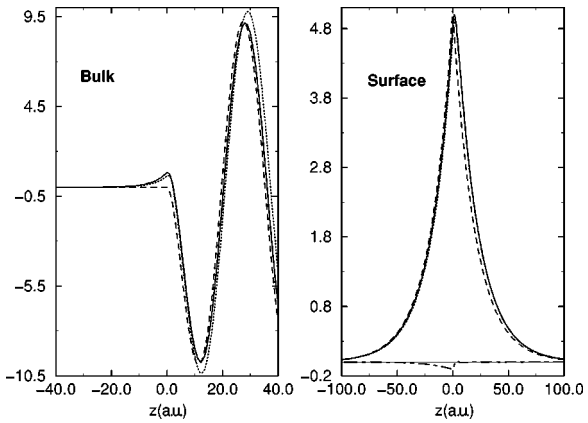

FIG. 1. Bulk and surface plasmon potentials for $Q=0.2$ a.u. (bulk) and $Q=0.05$ a.u. (surface) according to Bechstedt (solid line), Inglesfield (dashed line), and RPA (dotted line). The dot-dashed curve gives the imaginary part of the potential in the RPA case.

RPA bulk and surface fluctuation potentials for $Q=0.2$ a.u. (bulk) and $Q=0.05$ a.u. (surface). Landau damping sets in at $Q=0.68$ a.u. We also show results from the Inglesfield potential, which agree reasonably well both for bulk and surface plasmons. The coupling constants in the two approaches differ typically by only a few percent. The good agreement implies that the interference terms in the polarization function, which are neglected in Bechstedt's model, are small. From Fig. 1 we also see that the imaginary part in the RPA surface plasmon potential is quite small.

Bulk plasmon satellite intensities integrated over core positions for the QM, the SC, and the BS convolution cases, are shown in Fig. 2 for various photoelectron energies. We see that the QM and SC results approach each other fairly quickly, and above, say, 3–4 a.u., the difference is insignificant, while at low energies like 2 a.u. there are substantial differences. The BS result, on the other hand, is grossly off until at very high energies of the order of keV. We note

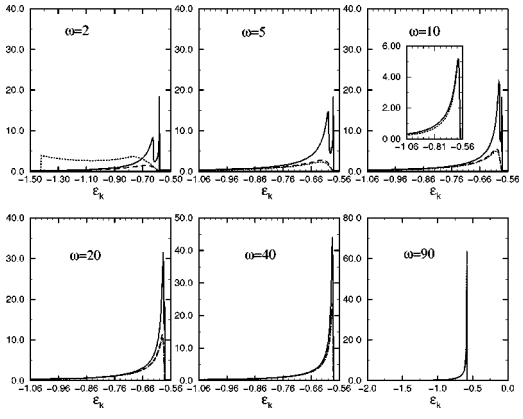

FIG. 2. Bulk plasmon satellite spectra for various photon energies, and for three different approaches: BS (solid curves), QM (dotted curves), and SC (dashed curves). At 90 a.u. no semiclassical results are shown. For the QM and SC results Inglesfield's fluctuation potential has been used. The inset shows bulk QM results, with Bechstedt's potential (dotted curve) and with Inglesfield's potential (solid curve). The photoelectron energies are with respect to the elastic peak position.

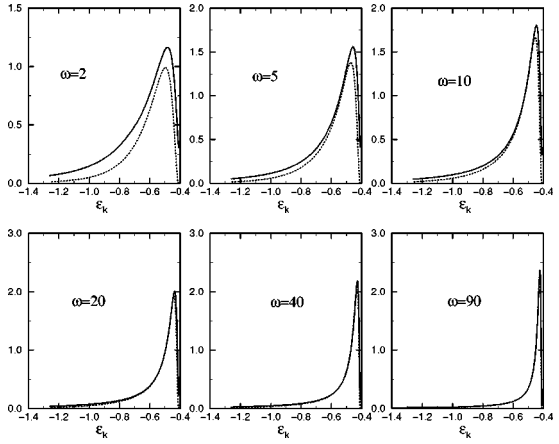

FIG. 3. Surface plasmon satellite spectra from Bechstedt's potential for various photon energies: QM (solid curves), and SC (dotted curves). The photoelectron energies are with respect to the elastic peak position.

the two peaks in the BS curves at lower energies. They arise from the intrinsic losses that start at the threshold energy ω_p, and the extrinsic losses that start at a slightly higher energy determined by momentum/energy selection rules. The inset in the panel for 10 a.u. shows a comparison between the results in the QM case using Bechstedt's and Inglesfield's potentials. The differences become smaller at higher energies, and slightly larger at lower energies. The sharp cutoff in the $\omega=2$ a.u. curve comes at $\varepsilon(\mathbf{k})=-(\omega-\phi-\varepsilon_F)=-1.43$ a.u.

Similar results are obtained for surface plasmon satellites, as shown in Fig. 3. In this case we can only show QM and

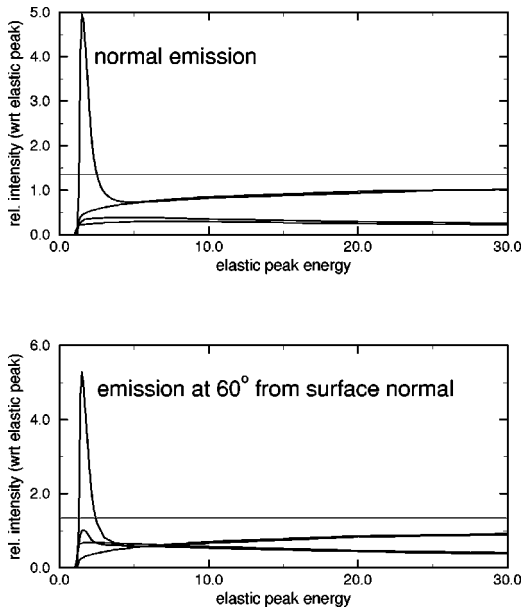

FIG. 4. Total intensity of bulk and surface plasmon satellites relative to the elastic peak weight, as a function of photon energy. In the top panel the two upper curves give bulk, and the two lower surface plasmons. The QM bulk curve shows a strong peak, while the SC curve is smooth. In the lower panel, the bulk curves change very little, while the QM surface plasmon curve has a small peak. The bulk modes are from Inglesfield's potential, and surface modes from Bechstedt's.

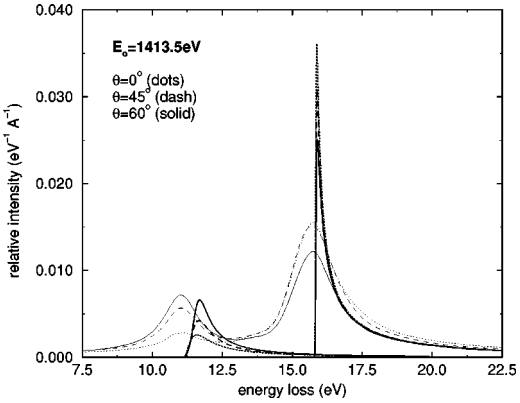

FIG. 5. Bulk and surface plasmon satellite spectra according to QM (bold curves) and Tougaard's (normal thickness) calculations, at a photonenergy of 1413.5 eV and three different angles. QM bulk plasmon from Inglesfield's and QM surface plasmon from Bechstedt's potential.

SC results, since we have not included any surface losses in our BS expression. The same trends as in the bulk case are observed, but the SC results agree better with the QM ones at low energies.

A clear illustration of how the satellite intensities in the QM and SC cases approach the BS limit is shown in Fig. 4, which is obtained by integrating the curves in Fig. 3 over energy. The QM and SC curves rapidly approach each other with increasing energy, and are already close at, say, 5 a.u. The bulk plasmon intensity approaches the BS high-energy limit [cf. Eq. (44)] of 1.35 (indicated by the dashed line) extremely slowly, and follows an $(\epsilon_{\mathbf{k}})^{-1/2}$ dependence as derived by Langreth and co-workers.[3] The surface plasmon intensity tends to zero at high energies, and also approaches this limit extremely slowly. At lower energies, the bulk curve has a pronounced maximum. As we remarked in Sec. II C 3, the $\Gamma(\omega)$ curve starts to rise strongly, due to plasmon damping, at about 1.1 a.u., and has a maximum at about 2 a.u. When ω is below 2 a.u. the elastic photoelectron thus has a stronger damping than the electrons in the satellite, and the relative satellite intensity is increased. This effect does not

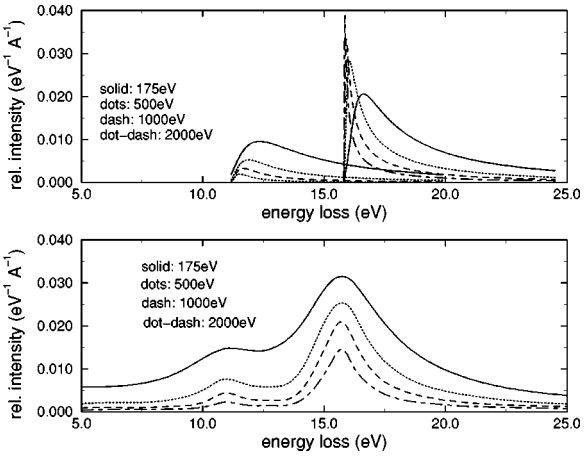

FIG. 6. Bulk and surface plasmon satellite spectra according to QM (top curves) and Tougaard (bottom curves), at various energies and normal emission. In the QM case the same potentials were used as in the previous figure.

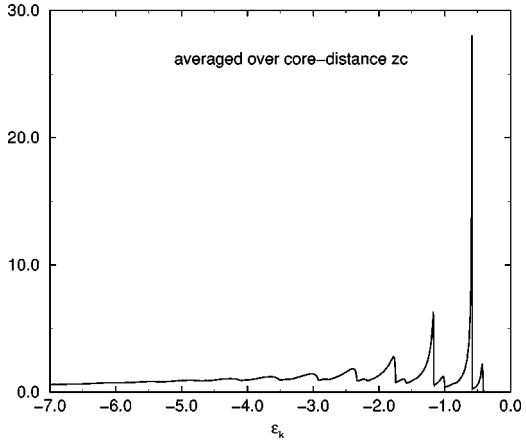

FIG. 7. Satellite spectra from the exponential expression, averaged over core positions, at the energy 50 a.u. Bechstedt's expression was used, and no particle-hole effects included.

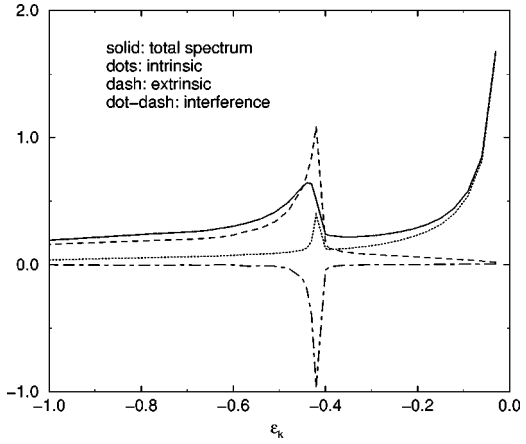

FIG. 9. RPA result from particle-hole pairs plus surface plasmons for the energy 5 a.u. and a core distance 20 a.u. Total spectrum, solid line; intrinsic spectrum, dots; extrinsic spectrum dashed line; and interference contribution, dot dashed line.

come in the SC approximation, where the damping is put in by hand, and is the same for the elastic peak and the satellites.

The surface plasmons can be excited only when the photoelectron is in the surface region, and with a long mean free path, this happens only during a small fraction of the path. The enhancement is thus expected to be much weaker for the surface plasmons. When the electron exits at an angle, as shown in the bottom panel of Fig. 4, a larger fraction of the mean free path is spent in the surface region, and surface losses are enhanced relative to bulk losses, and we then actually also have a small maximum in the surface contribution. In both cases the surface plasmon intensities are weaker than the bulk ones.

We have neglected the reabsorption contribution in Eq. (17). The results in Ref. 7 (which, however, did not include all reabsorption contributions) indicate a moderate increase in the elastic peak, and thus a reduction in the relative satellite intensity. A stronger reason, however, to expect the curiously large peak to be reduced is our neglect of elastic scattering, and also of impurity and phonon scattering. A small residual damping of 0.05 a.u. put in by hand removes most of the peak. Still, it is reasonable to expect some peaking at this energy to occur.

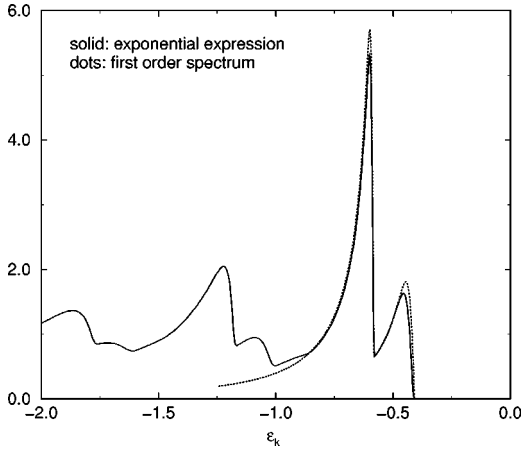

FIG. 8. Same as in Fig. 7, but for 10 a.u., and with the large loss region excluded.

Results from the Tougaard approach are shown in Figs. 5 and 6, and compared with our QM results. Figure 5 shows surface and bulk plasmon satellite spectra at various emission angles and at a high photon energy (1413.5 eV), where the agreement should be good. The overall features are similar, but there seems to be a non-negligible difference in strength, which we attribute to the different approximations of the dielectric functions. In both cases the surface plasmon satellite is clearly smaller than the bulk satellite for all emission angles.

The surface plasmon satellite becomes stronger as the angle of emission is increased, while the intensity of the bulk plasmon satellite goes down slightly, and the shapes of the satellites do not change much. In Fig. 6 we compare the dependence of the satellite spectra as a function of photon energy for normal emission. Here we consider total, not relative intensities. The trends roughly agree. The surface contribution decreases relative to the bulk one, and the bulk peak becomes sharper with increasing energy. The large broadening in the Tougaard curves, however, makes a quantitative comparison difficult.

In the last four figures we give results from the exponential expression in Eq. (36). Figure 7 shows results for the satellite spectrum at a rather high energy, 50 a.u., obtained

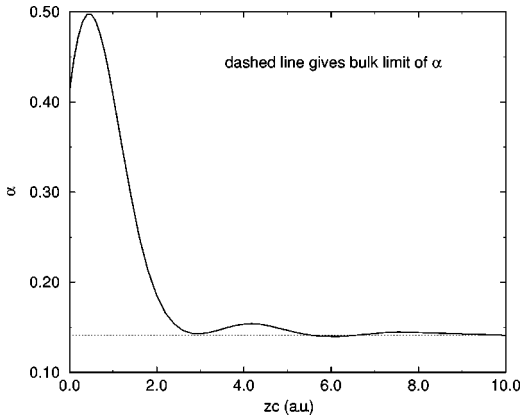

FIG. 10. Singularity index α as a function of core position. The dashed line gives the bulk limit of α.

with only surface and bulk plasmon, but not electron-hole, contributions included. The first, rather weak peak, comes from surface plasmon losses. Then follows a sequence of multiple bulk plasmon loss peaks, each followed by a weak surface loss peak. The double surface loss peak is marginally visible. A blow up of the threshold region at a somewhat lower energy, 10 a.u., is shown in Fig. 8, where we also compare with the first-order spectrum. The two spectra are identical out to the onset for two surface losses, except for the different treatment of the damping. In the exponential expression, Eq. (36), the damping comes from the integral $\int \beta(k,\omega')d\omega'$, which only asymptotically equals the exponent of the prefactor in Eq. (34), $a+\tau_0 z$.

Results from an RPA calculation, which include particle-hole pairs, are shown in Figs. 9 and 10. In Fig. 9 the energy is 5 a.u., and the core distance 20 a.u. The bulk plasmon contribution is not included. The different contributions to the total spectrum, the intrinsic, the extrinsic and the interferences parts are shown separately. We see that out to, say, 2 eV the intrinsic part dominates.

At the surface plasmon peak the intrinsic part is fairly small, and the extrinsic and interference parts strongly cancel. We also see that interference effects are important only in a narrow region at the peak of the surface plamon, and in particular they are very small in the quasiparticle tail. Since the intrinsic contribution dominates at threshold we can obtain an energy-independent singularity index α by fitting our numerical results to a power-law $\omega^{-(1-\alpha)}$, in a narrow region at threshold. The smallness of the interference contribution in the quasi-particle tail indicates that a BS convolution may work well here.

Results for different core distances are shown in Fig. 10. We see that we have to go to a distance of about 6 a.u. before the bulk asymptotic limit is reached. The coupling function $V_q(z)$ [cf. Eq. (31)] behaves like $-qz^2/2$ for small z. Thus $V_q(0)=0$, which leads to $\alpha=0$, the vanishing of all satellites, and a δ-function quasiparticle line. This unrealistic result depends on our neglect of the possibility for backscattering of the photoelectron, see remarks just before Eq. (26). Thus the behavior of α for very small z is unrealistic. We can, however, conclude that α is enhanced close to the surface. A more detailed estimate could be made fairly easily.

V. CONCLUDING REMARKS

We have studied three different levels of approximation for describing the photoemission current. In the quantum-mechanical approach (QM, Sec. II B–II D) we have an electron fully quantum-mechanically coupled to bosons, which represent electron-hole and plasmon excitations. In the semiclassical approach (SC, Sec. II F) the electron moves on a trajectory with a given velocity, and we evaluate the losses from the corresponding time-dependent perturbation by a quantum-mechanical calculation. Finally in the Berglund-Spicer approach (BS, Sec. II E) we convolute the intrinsic spectrum with an energy loss function. In the SC and BS cases we found exact solutions on an exponential form. The QM case cannot be solved exactly, but we find an exponential form, which reproduces the main features of the exact solution (cf. Sec. II D), and also of experiment (cf. Figs. 7 and 9 with experimental data in Pardee *et al.*[32] Note that we use atomic units, e.g., energy unit=27.2 eV). The QM and SC expressions are very similar and have a square of the sum of amplitudes for the extrinsic and intrinsic terms, while in the BS case we have a sum of the intensities from the extrinsic and intrinsic contributions. One can question how accurately our quasiboson model represents reality, but we believe it is the best model presented so far, which also has been quantitatively evaluated in detail.

The most important result is that the quasi-particle asymmetric line is found to follow the expected power law for several eV, and here is determined solely by the intrinsic term (cf. Fig. 9). From this one may guess that the widths and asymmetries of valence electron quasiparticles also are intrinsic effects given by the one-electron spectral function. The asymmetry index α depends on how far from the surface the atom sits, and is strongly enhanced close to the surface (cf. Fig. 10).

Another important result is the energies when QM becomes well represented by SC, and when SC (and thus QM) becomes well represented by BS (cf. Figs. 2–4). The first energy is approximately 5 a.u., while the second is say 50 a.u. (if we require, say, a 90% agreement). However already at, say, 20 a.u. the SC and BS cases give similar curves for the satellites, mainly differing by a scale factor.

For the effect of extrinsic scattering in the say, 5-eV-wide range, which is important for strongly correlated systems, it is hard to make any guesses from our present results. In this case the incoherent part is supposed to have important contributions from more short-range interactions, while for our model system the incoherent part was dominated by fairly sharp plasmon peaks coming from long-range interactions. This difference could make the approach to the sudden (=BS) limit much faster for strongly correlated systems without any pronounced plasmon excitations.

That we have a close relation between the QM and SC cases was indicated in an early work by Ashley and Ritchie.[34] The classical probability of having n collisions when the particle has traveled a distance z is given by the Poisson distribution,

$$P_n(z)=\frac{1}{n!}\left(\frac{z}{\lambda}\right)^n e^{-z/\lambda}.$$

They studied the same quasiboson Hamiltonian as in our paper, and showed that under certain conditions the quantum treatment also gives this Poisson distribution. However, they only derived the probability of having a certain number of energy losses, not of losing a certain amount of energy.

Fluctuation potentials have been widely used for a long time. Here we put them on a rigorous basis by relating them to the exact, and even more important, to the RPA dielectric response function. In the RPA case we find that formally we can define (and, in principle, use) fluctuation potentials also for the electron-hole continuum, and not only for the plasmon contributions. The form of the electron-hole potential $V^t(\mathbf{r})$, Eq. (52), is physically appealing. It shows explicitly that we work with a dynamically screened potential (with on-shell energies). In the usual Green's function expansions we also have a dynamically screened potential, $W(\omega)$. However in this case we integrate $W(\omega)$ over ω, and $W(\omega)$ is practically unscreened in some energy ranges.

To motivate our quasiboson model we study the high-energy limit, and find that it can be exactly represented by having a coupling between the photoelectron and density fluctuations. This is of course not much support when we want to discuss the fairly low energies, say, 5 a.u., where we go from QM to SC, and even less when we try to evaluate the strong relative enhancement in the satellite intensities at, say, 2 a.u. (cf. Fig. 4). A stronger argument for the quasiboson picture is probably that it makes physical sense, and that it has been successfully used before, both for the coupling to plasmons[28] and to phonons.[15]

Langreth and co-workers[3] have presented comprehensive formal discussions of photoemission. For more detailed considerations they turned to a similar quasiboson model as used in our work. However, they took a simpler coupling function [Eq. (12) in the second reference of Ref. 3], and they neglected the bulk and surface plasmon dispersions. They also made further approximations that reduced their expressions to the SC limit. We confirm their conclusion that the deviation from the BS result goes as $(\epsilon_{\mathbf{k}})^{-1/2}$ for large $\epsilon_{\mathbf{k}}$. It would be very interesting, but not simple, to find out how the choice of diagrams of Langreth and co-workers or Almbladh[5] are related to our model.

We have studied a very simple model case since our main purpose is to get a qualitative understanding of the relation between photoemission and the spectral function. Our approach is, however, general, and the one-electron Hamiltonian *h* can stand for a real solid with a surface. This case can be treated by taking the ionic potentials as perturbations, and calculating elastic scattering. We have used a constant self-energy. A possible next step is to evaluate the self-energy using fluctuation potentials. The effects of elastic scattering should actually be very important as discussed in an early paper by Tougaard and Sigmund.[35] A related approach can also be used for electron scattering.[27]

ACKNOWLEDGMENTS

A preliminary version of this work was presented at a workshop on Photoemission Lineshapes: the Sudden Approximation and Beyond, at the Institute of Theoretical Physics in Santa Barbara, April 1997. Constructive discussions, particularly with Jim Allen, Olle Gunnarsson, Walter Kohn, David Langreth, and Jerry Mahan, are gratefully acknowledged. We also thank Jeroen van den Brink and John Wilkins for a critical reading of the manuscript.

APPENDIX A: HIGH-ENERGY LIMIT OF PHOTOEMISSION

The general expression for photoemission was given in Eqs. (1) and (2). We follow Chew and Low[36] and rewrite the final state as

$$|\Psi_{\mathbf{ks}}\rangle = c_{\mathbf{k}}^{\dagger}|N-1,s\rangle + \frac{1}{E-H-i\eta} V_{CL}|N-1,s\rangle,$$

$$V_{CL} = [H, c_{\mathbf{k}}^{\dagger}] - \epsilon_{\mathbf{k}} c_{\mathbf{k}}^{\dagger}.$$

Evaluating the commutator we have

$$[H, c_{\mathbf{k}}^{\dagger}] = \sum_{\mathbf{k}_1} c_{\mathbf{k}_1}^{\dagger} h_{\mathbf{k}_1\mathbf{k}} + \frac{1}{2}\sum_{\mathbf{k}_1\mathbf{k}_2\mathbf{k}_3} \langle \mathbf{k}_1\mathbf{k}_2||v||\mathbf{k}\mathbf{k}_3\rangle c_{\mathbf{k}_1}^{\dagger} c_{\mathbf{k}_2}^{\dagger} c_{\mathbf{k}_3},$$

where $\langle \mathbf{k}_1\mathbf{k}_2||v||\mathbf{k}\mathbf{k}_3\rangle$ is an antisymmetrized Coulomb matrix element. We add and subtract a term

$$\sum_{\mathbf{k}_1\mathbf{k}_2\mathbf{k}_3} c_{\mathbf{k}_1}^{\dagger} \langle \mathbf{k}_1\mathbf{k}_2||v||\mathbf{k}\mathbf{k}_3\rangle \langle N-1,s|c_{\mathbf{k}_2}^{\dagger} c_{\mathbf{k}_3}|N-1,s\rangle$$

and choose the one-electron basis to diagonalize the HF-like one-electron Hamiltonian,

$$h_{\mathbf{k}_1\mathbf{k}} + \sum_{\mathbf{k}_2\mathbf{k}_3} \langle \mathbf{k}_1\mathbf{k}_2||v||\mathbf{k}\mathbf{k}_3\rangle \langle N-1,s|c_{\mathbf{k}_2}^{\dagger} c_{\mathbf{k}_3}|N-1,s\rangle.$$

For the continuum states we use scattering states. Since we have scattering states, the diagonal element must equal the free-electron energy $\epsilon_{\mathbf{k}}$. The $\epsilon_{\mathbf{k}} c_{\mathbf{k}}^{\dagger}$ terms in V_{CL} then cancel, and we have

$$V_{CL} = \sum_{\mathbf{k}_1\mathbf{k}_2\mathbf{k}_3} c_{\mathbf{k}_1}^{\dagger} \langle \mathbf{k}_1\mathbf{k}_2||v||\mathbf{k}\mathbf{k}_3\rangle \times \left(\frac{1}{2} c_{\mathbf{k}_2}^{\dagger} c_{\mathbf{k}_3} - \langle N-1,s|c_{\mathbf{k}_2}^{\dagger} c_{\mathbf{k}_3}|N-1,s\rangle \right).$$

We now discuss which are the dominant terms when the photoelectron has a high energy.

In the last term the states $\mathbf{k}_2$ and $\mathbf{k}_3$ must have limited energies, since the state $|N-1,s\rangle$ has a limited range of virtual one-electron energies. Further $\mathbf{k}_1$ must have a large energy, otherwise the matrix element $\langle \mathbf{k}_1\mathbf{k}_2||v||\mathbf{k}\mathbf{k}_3\rangle$ becomes small.

In the first term $c_{\mathbf{k}_3}$ must have a limited energy since it works on $|N-1,s\rangle$. Thus one of $\mathbf{k}_1$ and $\mathbf{k}_2$ must have a limited energy, and one a high energy (since $\mathbf{k}$ has a high energy), otherwise the matrix element $\langle \mathbf{k}_1\mathbf{k}_2||v||\mathbf{k}\mathbf{k}_3\rangle$ becomes small. The first term is symmetric in $\mathbf{k}_1$ and $\mathbf{k}_2$, and we can thus choose $\mathbf{k}_1$ to have a high energy, and omit the factor $\frac{1}{2}$.

We denote states with a high energy by $\mathbf{k}$ and with a limited energy by $\mathbf{l}$, and have

$$V_{CL} \cong \sum_{\mathbf{k}_1\mathbf{l}_1\mathbf{l}_2} c_{\mathbf{k}_1}^{\dagger} \langle \mathbf{k}_1 l_1||v||\mathbf{k} l_2\rangle \times (c_{\mathbf{l}_1}^{\dagger} c_{\mathbf{l}_2} - \langle N-1,s|c_{\mathbf{l}_1}^{\dagger} c_{\mathbf{l}_2}|N-1,s\rangle).$$

Again utilizing the properties of the Coulomb matrix elements we can write (where we have dropped the small exchange part in the antisymmetrized Coulomb matrix element)

$$|\Psi_{\mathbf{ks}}\rangle = \left[1 + \frac{1}{E-H-i\eta} V\right] c_{\mathbf{k}}^{\dagger}|N-1,s\rangle, \qquad \text{(A1)}$$

$$V = \sum_{\mathbf{k}_1\mathbf{k}_2}^{fast} \sum_{\mathbf{l}_1\mathbf{l}_2}^{slow} c_{\mathbf{k}_1}^{\dagger} c_{\mathbf{k}_2} \langle \mathbf{k}_1\mathbf{l}_1|v|\mathbf{k}_2\mathbf{l}_2\rangle$$

$$\times[c^\dagger_{\mathbf{l}_1}c_{\mathbf{l}_2}-\langle N-1,s|c^\dagger_{\mathbf{l}_1}c_{\mathbf{l}_2}|N-1,s\rangle]. \tag{A2}$$

We can rewrite V in terms of the density operator,

$$\rho(\mathbf{r})=\sum_{\mathbf{l}_1\mathbf{l}_2}\psi^*_{\mathbf{l}_1}(\mathbf{r})\psi_{\mathbf{l}_2}(\mathbf{r})c^\dagger_{\mathbf{l}_1}c_{\mathbf{l}_2}$$

and have

$$V=\sum_{k_1k_2}^{fast}c^\dagger_{\mathbf{k}_1}c_{\mathbf{k}_2}\int\psi^*_{\mathbf{k}_1}(\mathbf{r})v(\mathbf{r}-\mathbf{r}')\times[\rho(\mathbf{r}')-\langle\rho(\mathbf{r}')\rangle]\psi_{\mathbf{k}_2}(\mathbf{r})d\mathbf{r}d\mathbf{r}'. \tag{A3}$$

We now have the expected result: *At high energies we can treat the photoelectron as a distinguishable particle interacting with the density fluctuations of the target system.*

In the high-energy limit we can further write the full Hamiltonian as

$$H=H_s+h+V, \tag{A4}$$

where H_s describes the solid with all the electron-electron interactions (only **l** operators), h the photoelectron (only **k** operators), and V [Eq. (A3)] is the interaction between the photoelectron and the solid. We have dropped terms in the full Hamiltonian containing Coulomb interactions with one or three fast electrons, since the involved Coulomb integrals are small. We have also dropped Coulomb interactions with four fast electrons since they do not contribute when H operates on $Vc^\dagger_{\mathbf{k}}|N-1,s\rangle$. Thus in a perturbation expansion of Eq. (A1) we can work with eigenstates of H_s+h, which form a product basis, $|s'\rangle|\mathbf{k}'\rangle$ (for simplicity we have written $|s'\rangle$ for $|N-1,s'\rangle$).

In an extended system we may think of an excited state $|s'\rangle$ as having a finite number of extended boson-type excitations. Since each boson excitation only changes the charge density by a term proportional to $(\text{volume})^{-1}$, we take $\langle s'|\rho(\mathbf{r})|s'\rangle=\langle 0|\rho(\mathbf{r})|0\rangle$, for all s'. In a one-electron theory the charge-density operator $\rho(\mathbf{r})$ creates electron-hole pairs. $\langle s'|\rho(\mathbf{r})|s''\rangle$ is then different from zero only when the state s' contains one more or one less electron-hole pair, say, t, than we have in s'' (the cases when an operator in one pair coincides with an operator in another pair are so rare that we can neglect them). With a finite number of pairs we can replace $\langle s'|\rho(\mathbf{r})|s''\rangle$ by $\langle t|\rho(\mathbf{r})|0\rangle$ or $\langle 0|\rho(\mathbf{r})|t\rangle$ The charge fluctuations $\langle t|\rho(\mathbf{r})|0\rangle$ determine the *charge fluctuation potentials*, Eq. (50), which can be chosen to be real. The approximations we have made are actually in accordance with RPA, where the excited states are built of electron-hole pairs, and no multielectron multiholes are considered,[37] and also with recent successful descriptions of exciton effects.[38,39]

The interaction V can be written

$$V=\sum_{\mathbf{k}_1\mathbf{k}_2}\sum_{s_1s_2}\int\langle\mathbf{k}_1|V^{s_1s_2}|\mathbf{k}_2\rangle|s_1\rangle\langle s_2|c^\dagger_{\mathbf{k}_1}c_{\mathbf{k}_2}, \tag{A5}$$

$$V^{s_1s_2}(\mathbf{r})=\int v(\mathbf{r}-\mathbf{r}')\langle s_1|\rho(\mathbf{r}')-\langle\rho(\mathbf{r}')\rangle|s_2\rangle d\mathbf{r}'.$$

With the approximations above, it is reasonable to replace the Hamiltonian H by an electron-boson model Hamiltonian,

$$H_s=\sum_t\omega_t a^\dagger_t a_t, h=\sum_{\mathbf{k}}^{unocc}\epsilon_{\mathbf{k}}c^\dagger_{\mathbf{k}}c_{\mathbf{k}},$$

$$V=\sum_{t\mathbf{k}_1\mathbf{k}_2}V^t_{\mathbf{k}_1\mathbf{k}_2}(a_t+a^\dagger_t)c^\dagger_{\mathbf{k}_1}c_{\mathbf{k}_2},$$

$$V^t_{\mathbf{k}_1\mathbf{k}_2}=\langle\mathbf{k}_1|V^t(\mathbf{r})|\mathbf{k}_2\rangle.$$

Here we have represented $|s_1\rangle\langle s_2|$ by $a^\dagger_t$ when s_1 has one boson t more than s_2, and by a_t when it has one less. All $V^{s_1s_2}$ where s_1 differs from s_2 by more than one boson excitation are neglected.

APPENDIX B: THE FLUCTUATION POTENTIALS CORRESPONDING TO THE RPA DIELECTRIC FUNCTION

In Eq. (49) we gave the exact formal expression for the screened potential W in terms of fluctuation potentials V^t, which can be taken as real. We will here show that also in the RPA, W can be written as in Eq. (49).

1. Regular case

We rewrite $W=v(1-Pv)^{-1}$ as

$$W=v(1-Pv)^{-1}(1-P^\dagger v)(1-P^\dagger v)^{-1}$$
$$=v(1-Pv-P^\dagger v+P^\dagger vPv)^{-1}-WP^\dagger W^\dagger.$$

We write P in Eq. (51) as P_1+iP_2, where P_1 and P_2 are Hermitian, which gives

$$W=W_1-WP_1W^\dagger+iWP_2W^\dagger,$$

where

$$W_1=v^{1/2}(1-2v^{1/2}P_1v^{1/2}+v^{1/2}P^\dagger vPv^{1/2})^{-1}v^{1/2}.$$

Both $W_1-WP_1W^\dagger$ and $WP_2W^\dagger$ are Hermitian, and thus their diagonal parts are real in any basis set. We choose a complete set of real functions $\{g_i\}$, and have

$$\text{Im}\langle g_i|W|g_i\rangle=\langle g_i|\text{Im}\,W|g_i\rangle=\langle g_i|WP_2W^\dagger|g_i\rangle.$$

From Eq. (51) it follows that

$$P_2(\mathbf{r},\mathbf{r}';\omega)=-\pi\sum_t\varphi_t(\mathbf{r})\varphi_t(\mathbf{r}')\delta(\omega-\omega_t),$$

where the functions $\{\varphi_t\}$ are chosen as real, which gives

$$\langle g_i|\text{Im}\,W|g_i\rangle=-\pi\sum_t|\langle g_i|W|\varphi_t\rangle|^2\delta(\omega-\omega_t).$$

We will now show that $\text{Im}\,W=\text{Im}\,W_{trial}$ where,

$$\mathrm{Im}\, W_{trial}(\mathbf{r},\mathbf{r}';\omega) = -\frac{\pi}{2}\sum_t \left[V^t(\mathbf{r})V^t(\mathbf{r}')^* + cc\right]\delta(\omega-\omega_t) \tag{B1}$$

with

$$V^t(\mathbf{r}) = \int W(\mathbf{r},\mathbf{r}';\omega_t)\varphi_t(\mathbf{r}')d\mathbf{r}'. \tag{B2}$$

Both Im W [cf. Eq. (49)] and Im W_{trial} are real, and they are both symmetric in $\mathbf{r}$ and $\mathbf{r}'$. Their difference, which we call $D(\mathbf{r},\mathbf{r}')$ is thus also real and symmetric. Further the diagonal elements of D are zero. We have, for arbitrary functions $f(\mathbf{r})$ and $g(\mathbf{r})$,

$$0 = \langle f+g|D|f+g\rangle = \langle f|D|g\rangle + \langle g|D|f\rangle = 2\langle f|D|g\rangle.$$

Hence all matrix elements of D are zero, and D itself must be zero. From Eq. (B1) we obtain, by using the Kramers-Kronig relation, the corresponding expression for W.

Finally we introduce the real functions $V_1^t = \frac{1}{2}(V^t + V^{t*})$ and $V_2^t = 1/2i(V^t - V^{t*})$, and have

$$\mathrm{Im}\, W_{trial}(\mathbf{r},\mathbf{r}';\omega) = -\pi\sum_t \sum_{i=1}^{2} V_i^t(\mathbf{r})V_i^t(\mathbf{r}')\,\delta(\omega-\omega_t). \tag{B3}$$

2. Singular cases

In RPA for an electron gas, $P_2(|\mathbf{q}|,\omega)$ is zero outside the parabolas in the $(|\mathbf{q}|,\omega)$ plane that limit the particle-hole excitations, as discussed in Sec. III A. In this region there are simply no particle-hole excitations $\omega_{\mathbf{k},\mathbf{q}} = \varepsilon_{\mathbf{k}+\mathbf{q}} - \varepsilon_{\mathbf{k}}$ ($\varepsilon_{\mathbf{k}+\mathbf{q}} \geqslant \varepsilon_F \geqslant \varepsilon_{\mathbf{k}}$), due to phase-space restrictions. As is well known, we still have contributions from this region in the $(|\mathbf{q}|,\omega)$ plane from plasmon excitations. Similarly for a solid with a surface, we can have singular bulk plasmon contributions in addition to those in Eq. (B3). To obtain these contributions we follow another approach.

Write W on a symmetrized form,

$$W = v^{1/2}(1 - v^{1/2}Pv^{1/2})^{-1}v^{1/2} \equiv v^{1/2}\tilde{\varepsilon}^{-1}v^{1/2}. \tag{B4}$$

The effective dielectric function $\tilde{\varepsilon}$ is symmetric. We solve for eigenvalues and eigenfunctions

$$\tilde{\varepsilon}(\omega)\varphi_i = \lambda_i(\omega)\varphi_i(\omega).$$

Taking the set $\{\varphi_i\}$ as orthonormalized, we have

$$\tilde{\varepsilon}(\mathbf{r},\mathbf{r}';\omega) = \sum_i \lambda_i(\omega)\varphi_i(\mathbf{r};\omega)\varphi_i(\mathbf{r}';\omega),$$

$$\tilde{\varepsilon}^{-1}(\mathbf{r},\mathbf{r}';\omega) = \sum_i \frac{1}{\lambda_i(\omega)}\varphi_i(\mathbf{r};\omega)\varphi_i(\mathbf{r}';\omega), \tag{B5}$$

$$W(\mathbf{r},\mathbf{r}';\omega) = \sum_i \frac{w_i(\mathbf{r};\omega)w_i(\mathbf{r}';\omega)}{\lambda_i(\omega)}, \quad w_i = v^{1/2}\varphi_i.$$

The fluctuation potentials $w_i(\mathbf{r};\omega)$ satisfy the equation

$$(1 - vP)w_i = \lambda_i(\omega)w_i. \tag{B6}$$

Equation (B5) gives a complete representation of W. It is, however, not on the spectral form we have in Eq. (49), except when $\lambda_i(\omega) = 0$ has a real pole. Assuming that we can take the functions w_i as real we have

$$\mathrm{Im}\, W(\mathbf{r},\mathbf{r}';\omega) = -\pi\sum_{im}\left[\frac{\partial\lambda_i(\omega)}{\partial\omega}\right]^{-1} w_i(\mathbf{r};\omega)w_i(\mathbf{r}';\omega) \times \delta(\omega-\omega_{im}).$$

We can now identify a fluctuation potential coming from a singular part of W as

$$V^{im}(\mathbf{r}) = \left|\frac{\partial\lambda_i(\omega)}{\partial\omega}\right|^{-1/2} w_i(\mathbf{r};\omega)\Bigg|_{\omega=\omega_{im}}. \tag{B7}$$

For bulk and surface plasmons i corresponds to $\mathbf{k}$ and $\mathbf{Q}$, respectively, and in the cases we discuss, there is only one root m for each i. For an electron gas the functions w_i are not real, but rather plane waves. However, we can then take a Fourier transform, and Eq. (B7) still holds. The presence of singular contributions is connected with having very simple models like the electron gas, and for a solid with band structure they do not appear. Still approximations of plasmon-pole type may be useful also for more complex systems.

In Sec. III D we also will need the charge fluctuations $\delta\rho_i$, which satisfy

$$(1 - Pv)\,\delta\rho_i = \lambda_i(\omega)\,\delta\rho_i, \quad w_i = v\,\delta\rho_i. \tag{B8}$$

APPENDIX C: HARMONIC OSCILLATOR WITH TIME-DEPENDENT POTENTIAL

In treating the semiclassical approximation (the trajectory approximation), we have a problem described by the Hamiltonian

$$H(t) = \sum_{\mathbf{q}} \left[\omega_{\mathbf{q}}a_{\mathbf{q}}^\dagger a_{\mathbf{q}} + V_{\mathbf{q}}(t)(a_{\mathbf{q}} + a_{\mathbf{q}}^\dagger)\right],$$

$$V_{\mathbf{q}}(t) = 0 \quad \text{for} \quad t \leqslant 0.$$

We first treat the problem with one oscillator, and can then easily obtain the solution for a sum of oscillators. The time evolution is written $|t\rangle = U(t)|0\rangle$, where $|0\rangle$ is the ground state of $H(0) = \omega a^\dagger a$. We have ($\hbar = 1$)

$$H(t) = \omega a^\dagger a + V(t)[a + a^\dagger] \Rightarrow i\frac{da(t)}{dt} = \omega a(t) + V(t),$$

$$a(t) = U(t)^\dagger a U(t) = e^{-i\omega t}[a - ig(t)],$$

$$g(t) = \int_0^t e^{i\omega t'}V(t')dt'.$$

The probability amplitude for the state $|t\rangle$ to have n excitations is

$$\langle n|t\rangle \equiv \frac{1}{\sqrt{n!}}\langle 0|a^n U(t)|0\rangle = \frac{1}{\sqrt{n!}}\langle 0|U(t)a(t)^n|0\rangle$$
$$= \frac{e^{-in\omega t}[-ig(t)]^n}{\sqrt{n!}}\langle 0|U(t)|0\rangle.$$

Using the fact that $\Sigma_n|\langle n|t\rangle|^2=1$, we have

$$P_n \equiv |\langle n|t\rangle|^2 = e^{-|g(t)|^2}\frac{|g(t)|^{2n}}{n!}. \tag{C1}$$

We are interested in the case when time goes to infinity, and denote $|g(\infty)|=g$. It is, further, convenient to introduce the energy distribution $P(\varepsilon)$,

$$P(\varepsilon)=\sum_n P_n \delta(\varepsilon - n\omega) = \frac{1}{2\pi}\int_{-\infty}^{\infty} e^{i\varepsilon t} e^{g^2[e^{-i\omega t}-1]}dt.$$

When we have many oscillators $\mathbf{q}$, each with a probability $P^{\mathbf{q}}_{n_{\mathbf{q}}}$ of having $n_{\mathbf{q}}$ excitations $\omega_{\mathbf{q}}$, we are interested in the energy distribution

$$P(\omega) = \sum_{n_{\mathbf{q}} n_{\mathbf{q}'} \cdots} (P^{\mathbf{q}}_{n_{\mathbf{q}}} P^{\mathbf{q}'}_{n_{\mathbf{q}'}} \cdots)\, \delta(\omega - n_{\mathbf{q}}\omega_{\mathbf{q}} - n_{\mathbf{q}'}\omega_{\mathbf{q}'} - \cdots)$$
$$= \frac{1}{2\pi}\int_{-\infty}^{\infty} e^{i\omega t} e^{\sum_{\mathbf{q}} |g^0_{\mathbf{q}}|^2[e^{-i\omega_{\mathbf{q}}t}-1]}dt, \tag{C2}$$

$$|g^0_{\mathbf{q}}| = \left|\int_0^{\infty} e^{i\omega_{\mathbf{q}}t} V_{\mathbf{q}}(t)dt\right|.$$

This is the result we need in Sec. II F.

[1] C. N. Berglund and W. E. Spicer, Phys. Rev. **136**, A1030 (1964).
[2] C. Caroli, D. Lederer-Rosenblatt, B. Roulet, and D. Saint-James, Phys. Rev. B **8**, 4552 (1973).
[3] J. J. Chang and D. C. Langreth, Phys. Rev. B **5**, 3512 (1972); **8**, 4638 (1973); D. C. Langreth in *Linear and Non-Linear Transport in Solids*, Vol. 17 of *NATO Advanced Study Institute Series B: Physics*, edited by J. Devreese and V. E. van Doren (Plenum, New York, 1976).
[4] P. Longe, P. Kiehm, and S. M. Bose, Phys. Rev. B **27**, 6000 (1983).
[5] C.-O. Almbladh, Phys. Scr. **32**, 341 (1985); Phys. Rev. B **34**, 3798 (1986)
[6] J. E. Inglesfield, Solid State Commun. **40**, 467 (1981); J. Phys. C **16**, 403 (1983).
[7] W. Bardyszewski and L. Hedin, Phys. Scr. **32**, 439 (1985).
[8] D. M. Newns, Phys. Rev. B **1**, 3304 (1970).
[9] F. Bechstedt, R. Enderlein, and D. Reichardt, Phys. Status Solidi B **117**, 261 (1983).
[10] E. Wikborg and J. E. Inglesfield, Phys. Scr. **15**, 37 (1977).
[11] P. J. Feibelman, C. B. Duke, and A. Bagchi, Phys. Rev. B **5**, 2436 (1972).
[12] A. G. Eguiluz, Phys. Rev. B **23**, 1542 (1981).
[13] J. Lindhard, K. Dan. Vidensk. Selsk. Mat. Fys. Medd. **28**, 8 (1954).
[14] R. A. Ferrell, University of Maryland Technical Report No. 485, 1965 (unpublished).
[15] A. A. Lucas, E. Kartheuser, and R. G. Badro, Phys. Rev. B **2**, 2488 (1970); M. Sunjic and A. A. Lucas, *ibid.* **3**, 719 (1971).
[16] A. C. Simonsen, F. Yubero, and S. Tougaard, Phys. Rev. B **56**, 1612 (1997).
[17] F. Flores, Nuovo Cimento B **14**, 1 (1973).
[18] L. Hedin, Phys. Rev. A **139**, A796 (1965).
[19] G. D. Mahan, *Many-Particle Physics* (Plenum, New York, 1981).
[20] M. L. Goldberger and K. M. Watson, *Collision Theory* (Wiley, New York, 1964).
[21] L. Hedin and S. Lundqvist in *Solid State Physics*, edited by Seitz *et al.* (Academic, New York, 1969), Vol. 23, p. 1.
[22] P. J. Feibelman and D. E. Eastman, Phys. Rev. B **10**, 4932 (1974).
[23] J. B. Pendry, Surf. Sci. **57**, 679 (1976).
[24] H. Feshbach, Ann. Phys. (N.Y.) **43**, 410 (1967).
[25] A more detailed analysis shows that the second term in $f(z)$ should be multiplied with a phase factor $e^{i\eta_1(k)}$, where $\eta_1(k)$ is the p phase shift for the atomic potential. In the calculations we have taken $\eta_1(k)=0$.
[26] L. Hedin, in *Recent Progress in Many-Body Theories*, edited by A. J. Kallio, E. Pajanne, and R. F. Bishop (Plenum, New York, 1988), Vol. 1, p. 307.
[27] T. Fujikawa and L. Hedin, Phys. Rev. B **40**, 11 507 (1989).
[28] C.-O. Almbladh and L. Hedin, *Handbook on synchr. rad.*, edited by E. E. Koch (North-Holland, Amsterdam, 1983), Vol. 1, pp. 607–904.
[29] D. Langreth, Phys. Rev. **182**, 973 (1969); Phys. Rev. B **1**, 471 (1970).
[30] L. Landau, J. Phys. (Moscow) **8**, 201 (1944).
[31] C. J. Tung and R. H. Ritchie, Phys. Rev. B **16**, 4302 (1977).
[32] W. J. Pardee, G. D. Mahan, L. Ley, F. R. McFeely, S. P. Kowalezyk, and D. A. Shirley, Phys. Rev. B **11**, 3614 (1975).
[33] E. Merzbacher, *Quantum Mechanics*, (Wiley, New York, 1970).
[34] X. Ashley and R. H. Ritchie, Phys. Rev. **174**, 1572 (1968).
[35] S. Tougaard and P. Sigmund, Phys. Rev. B **25**, 4452 (1982).
[36] G. F. Chew and F. E. Low, Phys. Rev. **101**, 1579 (1956).
[37] K. Sawada, K. A. Brueckner, N. Fukuda, and R. Brout, Phys. Rev. **108**, 507 (1957).
[38] S. Albrecht, G. Onida, and L. Reining, Phys. Rev. B **5**, 10 278 (1997).
[39] L. X. Benedict, E. L. Shirley, and R. B. Bohn, Phys. Rev. B **57**, R9385 (1998).